polymer reviews

A kinetic model for olefin polymerization in high-pressure tubular reactors: a review and update

R. C. M. Zabisky* and W.-M. Chan
Technology Center, Poliolefinas S A, Av. Presidente Costa e Silva 400, Santo André, São Paulo, Brazil 09270

P. E. Gloor and A. E. Hamielec
McMaster Institute for Polymer Production Technology, Department of Chemical Engineering, McMaster University, Hamilton, Ontario, Canada L8S 4L7
(Received 4 August 1990; revised 6 June 1991; accepted 2 July 1991)

Free-radical copolymerization in high-pressure tubular reactors is considered. Kinetic mechanisms to describe the polymerization rate and polymer properties, including copolymer composition, molecular weight, branching frequencies, melt flow index and polymer density, have been proposed. Based upon this kinetic scheme, a mathematical model has been derived and implemented as a computer program to simulate commercial tubular reactors. For calculation of molecular-weight averages, the method of moments is used in conjunction with pseudo kinetic rate constants to allow for copolymerization. The model parameters were fitted to industrial data to give useful steady-state simulation software, allowing for multiple feed points, multiple initiators (including oxygen) and non-isothermal polymerization. The effects of the pulse valve and the product cooler are incorporated. Comparisons are made between the model predictions and industrial data. A new approach and considerations for solving the moment closure problem are presented.

(Keywords: high-pressure polyethylene; free-radical copolymerization; tubular reactor; moment closure technique)

INTRODUCTION

Low-density polyethylene (LDPE) and copolymers are widely used for a large variety of applications and commonly produced in either autoclave-type vessels or tubular reactors. This work concentrates on the production of LDPE and copolymers in tubular reactors with the objective to develop a mechanistic model to describe the important chemical and physical phenomena that occur in this type of polyethylene reactor. This model is then used as the basis for a computer program (TUBULAR) to simulate the steady-state production of LDPE and copolymers in tubular reactors.

The computer model predicts the temperature, pressure and fractional conversion profiles along the reactor as well as the final product quality. The properties of interest are the copolymer composition, molecular-weight averages, branching frequencies, melt viscosity and polymer density. The computer simulation can then be used to develop new products and improved methods of making existing products. Safety calculations can easily be performed using the simulation model. By incorporating the kinetics of free-radical copolymerization into the model, we can simulate a multitude of new copolymers to determine, at least as a first estimate, the ideal proportions of each monomer in the feed to yield the desired copolymer product.

* To whom correspondence should be addressed

A mathematical model to describe high-pressure tubular reactors has been developed. This model is based upon proposed kinetic mechanisms for the copolymerization, and upon a knowledge of the reactor flow and temperature characteristics.

There have been several tubular reactor models presented in the literature (as will be described at the appropriate points throughout this work and in Appendix 3), many with some shortcoming, lacking comparisons with experimental or industrial data or only for homopolymerization. Many of these models neglect the effects of the pulse valve and the product cooler. This paper endeavours to present a comprehensive model and give actual comparisons with industrial data to support the theory.

REACTION KINETICS FOR COPOLYMERIZATION

This model attempts to account for the important elementary reactions that are likely to occur in the tubular reactor via the terminal model for copolymerization (penultimate effects are neglected). The reactions to be considered are presented below. The analysis is simplified without any loss of rigour by using pseudo kinetic rate constants[20,49]. Finally, the model parameter estimation was based on the use of valid literature and plant data. Of note is the fact that the values for the

0032-3861/92/112243-20

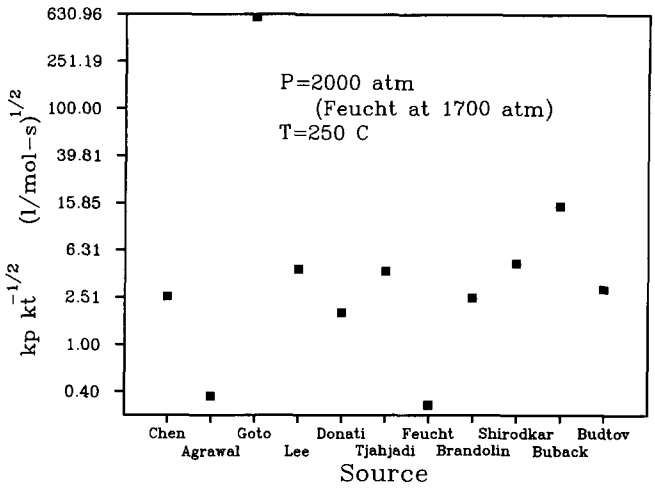

Figure 1 A sampling of the rate parameters for ethylene polymerization, from various sources

kinetic rate constants, reported in the literature, seem to vary over a wide range[18]. If we just consider the rate of polymerization, the ratio $k_p/k_t^{1/2}$ is important. *Figure 1* shows this ratio as reported by several authors. The range over which this varies is quite apparent, although, to be fair, it must be pointed out that these values arise from different measurement techniques and modes of initiation.

The elementary reactions

The appropriate reactions considered are listed below. The terminal model is assumed to be adequate to describe this kind of polymerization, i.e. the rates of reaction depend only upon the monomer unit on which the radical centre is located, and thus penultimate effects are ignored. The reactions include initiation, propagation, bimolecular termination, transfer to small molecules and polymer, backbiting, β-scission, reactions with terminal double bonds, and explosive decomposition of monomer and polymer.

Initiation. The decomposition of peroxide initiator, I, to form free radicals R:

$$\mathrm{I} \xrightarrow{k_d} n\mathrm{R}$$

where n is the number of radicals formed per initiator molecule, usually two. It is assumed that each radical formed has the same reactivity.

Oxygen initiation of ethylene polymerization was first reported by Fawcett *et al.*[14], and has been used commercially in both tubular and vessel-type reactors. It is well known that oxygen also acts as an inhibitor in free-radical polymerizations at lower temperatures. Ehrlich and Pittilo[12] studied the O_2 effect and found definite pressure and temperature boundaries between the inhibition and the initiation regimes. On the other hand, Gierth[16] found a gradual transition from one regime to the other. Certainly these phenomena are quite complex. Oxygen may react with radicals or monomer to form polymeric peroxides. These peroxides may then decompose to initiate the polymerization[32]. Several authors, including Thies[47], have tried to model O_2 initiation by assuming the overall second-order reaction:

$$\mathrm{O_2} + \mathrm{M} \xrightarrow{k_{dO_2}} 2\mathrm{R}$$

neglecting the inhibition reactions, with moderate success.

In tubular reactor *simulations*, the tendency is to give a sharp temperature peak, at the end of each reaction zone, as the oxygen burns out. In practice, a rounded peak is observed for oxygen initiation. Hollar and Ehrlich[25] attempted to produce a rounded peak by incorporating a thermal self-initiation reaction for ethylene[6]. Even so, the peak was not rounded but sharp with a gradual drop, due to this self-initiation. They found that the oxygen had to behave as two separate initiators, one fast and one much slower. In the present work it was found that a first-order oxygen initiation rate does not explain both the correct initial temperature rise and the rounding off at the peak. We agree that the oxygen acts as two separate initiators, one fast (responsible for the heat kick for the initial temperature rise) and one slower (responsible for the rounded peak). For these reasons it was decided that the oxygen phenomena must be examined more closely.

Tatsukami, Takahashi and Yoshioka[46] have studied the oxygen initiation of ethylene and postulated the additional reaction:

$$\mathrm{R} + \mathrm{O_2} \xrightarrow{k_r} \text{deactivated products and peroxides} \qquad \textit{inhibition}$$

These reactions account for the initiation and the inhibition effects of oxygen, but not for the slow initiation at high temperatures responsible for the rounded peak. To explain this, Brandolin *et al.*[5] assumed that the initiation rate was of order 1.1 with respect to oxygen. We chose to try a less empirical method whereby some of the peroxides formed by the inhibition reaction can decompose to initiate the reaction further. Thus the oxygen effect can be modelled with the additional reaction:

$$\mathrm{RO_2} \xrightarrow{k_{dp}} 2\mathrm{R} \qquad \textit{slow initiation}$$

where RO_2 represents the products of the inhibition reaction that are peroxides, and R denotes some possible polymeric end group.

As mentioned previously, monomer may also thermally combine to form a radical type i. Although this reaction is thought to be very minor for ethylene[32], it may be significant at higher temperatures, causing reactor runaways[25]. Buback[6] found this reaction to be third order in ethylene. Since we do not know the actual mechanism for this reaction, we shall retain it as an overall third-order reaction:

$$3\mathrm{M}_i \xrightarrow{k_{th}} \mathrm{R}_i$$

Propagation. Propagation of monomer type i with radicals of length r ending in monomer type j:

$$\mathrm{R}_j(r) + \mathrm{M}_i \xrightarrow{k_{pji}} \mathrm{R}_i(r+1)$$

Termination. Bimolecular termination reactions between two radicals to form one or two *dead* polymer chains, either by combination:

$$\mathrm{R}_i(r) + \mathrm{R}_j(s) \xrightarrow{k_{tcji}} \mathrm{P}(r+s)$$

or by disproportionation:

$$\mathrm{R}_i(r) + \mathrm{R}_j(s) \xrightarrow{k_{tdji}} \begin{cases} \mathrm{P}^{=}(r) + \mathrm{P}(s) \\ \text{or} \\ \mathrm{P}^{=}(s) + \mathrm{P}(r) \end{cases}$$

The disproportionation reaction forms a *dead* chain with a terminal double bond, denoted by the superscript =.

Transfer reactions. Transfer of reactivity to small molecules:

(i) Transfer to monomer. Transfer of reactivity from radical type j to a monomer type i to form a monomer transfer radical and a *dead* polymer chain:

$$R_j(r) + M_i \xrightarrow{k_{fmji}} R_i^{=}(1) + P(r)$$

The transfer radical with propagation will have a double bond and thus this radical will become polymer with a terminal double bond.

(ii) Transfer to chain transfer agent, modifier or solvent. Transfer of reactivity from radical type j to chain transfer agents, TS, to form a *dead* polymer chain and the transfer radical, TS*:

$$R_j(r) + TS \xrightarrow{k_{fts j}} TS^* + P(r)$$

It is assumed that TS* has the same reactivity as polymer radicals. The chain transfer agent will not affect the rate of reaction when bimolecular termination is chemically controlled, but can reduce the polymerization rate when termination is diffusion-controlled and chain-length-dependent.

β-scission of terminal radicals. Terminal radicals may undergo β-scission[11,36] at the high temperatures of polymerization forming a *dead* polymer chain and a radical of unit length:

$$R_j(r) \xrightarrow{k_\beta} P^{=}_{i\,or\,j}(r-1) + R_j(1)$$

It is assumed that this will not affect the rate of polymerization, but of course would reduce the molecular weight of the product.

Reactions with internal radical centres

An internal radical centre is a radical located on a backbone carbon atom and is formed by two reactions: (i) transfer to polymer and (ii) backbiting. These internal radical centres can, in theory, undergo all of the reactions that chain-end radicals do. Propagation leads to branches, the type depending upon the formation mechanism. Transfer to polymer leads to long chain branches, and backbiting leads to short chain branches. In addition, these internal radicals could undergo a β-scission reaction to form two smaller chains.

Transfer to polymer leading to long chain branching (LCB). This reaction involves the transfer of reactivity from radical type j to an i type monomer unit in a *dead* polymer chain to form a radical with the active centre somewhere along the chain. In the presence of monomer, propagation leads to long chain branching:

$$R_j(r) + P_i(s) \xrightarrow{k_{fpji}} R_i'(s) + P(r)$$

and then propagation:

$$R_i'(s) + M_j \xrightarrow{k_{pij}} R_j(s+1) \qquad LCB$$

where R′ denotes an internal radical. With excess monomer, we can write this two-step reaction as a single overall reaction:

$$R_j(r) + P_i(s) \xrightarrow{K_{LCB}} R(s)_{branched} + P(r)$$

Backbiting leading to short chain branching (SCB). For the formation of short chain branches via backbiting, the radical activity is transferred to a site along the same chain, and this site may propagate leaving a short chain branch:

$$R_j(r) \xrightarrow{k_{bji}} R_i'(r)$$

and then propagation:

$$R_i'(r) + M_j \xrightarrow{k_{pij}} R_j(r+1) \qquad SCB$$

As with long chain branching, we can write this two-step reaction as a single overall reaction:

$$R(r) \xrightarrow{K_{SCB}} R(r)_{branched}$$

β-scission of internal radical centres. In addition to the propagation reactions, internal radicals may undergo β-scission to form two smaller radical and *dead* polymer chains, one with a terminal double bond:

$$R_j'(r) \xrightarrow{k'_{\beta j}} \begin{cases} P^{=}(s) + R_{j\,or\,i}(r-s) \\ \text{or} \\ P^{=}(r-s) + R_{j\,or\,i}(s) \end{cases}$$

This reaction is actually a two-step reaction, whereby the first step is the attack of a *dead* polymer chain by a radical, forming an internal radical, the second step being the scission reaction. One can write this as an overall reaction of the form:

$$R_j(q) + P(r) \xrightarrow{K_\beta} \begin{cases} P^{=}(s) + R_{i\,or\,j}(r-s) + P(q) \\ \text{or} \\ P^{=}(r-s) + R_{i\,or\,j}(s) + P(q) \end{cases}$$

Terminal double-bond reactions

The reactions of termination by disproportionation, β-scission and transfer to monomer produce chain ends that have double bonds. These double bonds might react with radicals, via a propagation-type reaction, producing internal radicals that can propagate to form long chain branches:

$$P_j^{=}(r) + R_i(s) \xrightarrow{k_{dbji}} R_j'(r+s)$$

Since for the type of polymerization being considered the conversion of monomer is usually low, the concentration of these terminal double bonds relative to the concentration of double bonds available as monomer is quite small. For this reason we shall neglect these terminal double-bond reactions.

Explosive decomposition

The thermal decomposition of monomer and polymer at high temperatures to form a variety of lower-molecular-weight products:

$$M_j \xrightarrow{k_{dcmj}} \text{carbon} + \text{hydrogen, etc.}$$

$$P(r) \xrightarrow{k_{dcp}} \text{carbon} + \text{hydrogen, etc.}$$

A reactor runaway usually results in a huge pressure

increase due to the rapid evolution of small molecules via these decomposition reactions.

KINETIC MODEL DEVELOPMENT

The mathematical model to describe the polymerization is presented below. *Figure 2* shows a schematic of the high-pressure process, and the elements enclosed by the broken line are included in this simulation model. Notice that this model considers the product cooler section (after the pulse valve) to be part of the reactor, as well as the pulse valve. It is well known from industrial practice that, by changing operating conditions in the process, the final polymer properties vary significantly, even though the synthesis conditions inside the reactor remain the same. A more detailed configuration of the proposed modelling system is shown in *Figure 3*.

The model includes mass, momentum and energy balances for a tubular reactor. We assume that the tubular reactor and the cooling jackets experience plug flow, i.e. there are no radial temperature or concentration gradients in the tube or jackets, and no axial mixing. The validity of these assumptions depends upon the L/D ratios, the fluid properties and the Reynolds numbers. Since the Reynolds number for these reactors is usually greater than 10000 (Chen *et al.*[8]), and the L/D ratios are very large, these assumptions should be valid. Fluid mechanical studies[10] seem to suggest that the axial mixing effect is of minor importance, and Yoon and Rhee[52] confirm this.

We also assume that the reaction mixture is homogeneous. There may be a polymer-rich phase precipitating very near the tube wall, where it is cooler. The reaction rates will be much different there, but we are neglecting this since resins produced in tubular reactors do not show the grainy film appearance, a typical characteristic of two-phase reaction polymer obtained in autoclave reactors. With these assumptions, the model should give reasonable predictions of the polymer quality, temperature and fractional conversion profiles along the reactor. Relaxing these assumptions would lead to greater model complexity with a small increase in accuracy.

The model is written using axial distance L as the independent variable. The equations will be solved in this form by integrating along the reactor length. We will consider mass balances on each species in the reactor, heat transfer from the reaction mixture to the cooling jacket, and the pulse valve effect is modelled last.

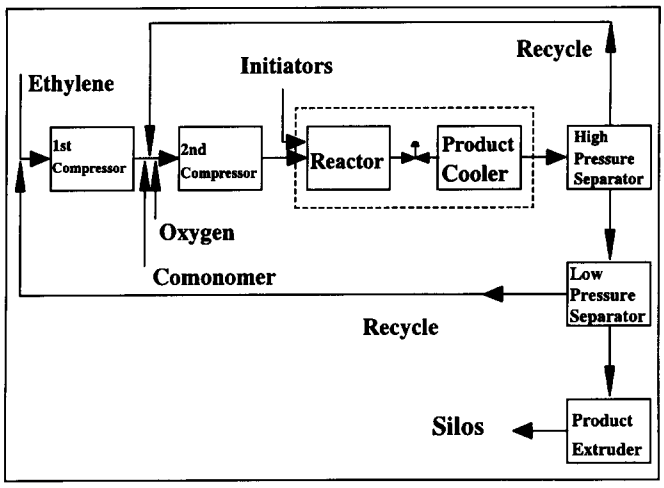

Figure 2 The process for synthesis of high-pressure polyethylene and copolymers

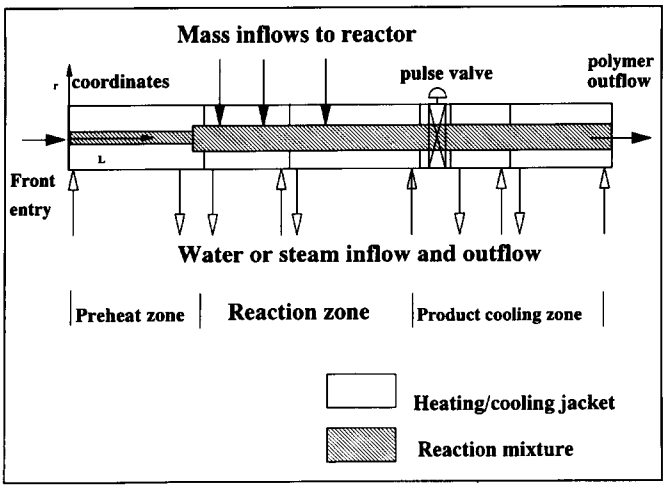

Figure 3 Schematic diagram of tubular reactor with multiple feed points

The pseudo kinetic rate constants

One can simplify the mathematical equations for a copolymerization by using pseudo kinetic rate constants. These rate constants are the rate constants for each elementary reaction weighted by the fraction of monomer or radical type in the reactor. Instead of writing down all the reactions between all monomer or radical types, we can formulate the equations in terms of the total monomer or radical concentrations. First we must calculate some fractions based upon the composition of the reactor contents, and the kinetic constants.

The reactivity ratios for propagation are defined as:

$$r_1 = k_{p11}/k_{p12} \tag{1}$$

$$r_2 = k_{p22}/k_{p21} \tag{2}$$

where k_{pij} is the elementary propagation rate constant for adding monomer type j to polymer radical of type i.

The mole fraction of each monomer type in the reaction mixture is given by:

$$f_1 = M_1/M \qquad f_2 = 1 - f_1 \tag{3}$$

where M_1 and M are moles of monomer of type 1 and the total moles of monomer, respectively.

The mole fraction of monomer type 1 chemically bound in the accumulated polymer (i.e. the copolymer composition) is given in two ways as follows. *Accumulated copolymer composition:*

$$\bar{F}_1 = \Psi_1/(\Psi_1 + \Psi_2) \qquad \bar{F}_2 = 1 - \bar{F}_1 \tag{4}$$

where Ψ_1 is moles of monomer 1 bound in polymer, and Ψ_1 and Ψ_2 can be found using a mass balance. *Instantaneous copolymer composition:*

$$F_1 = \frac{(r_1 - 1)f_1^2 + f_1}{(r_1 + r_2 - 2)f_1^2 + 2(1 - r_2)f_1 + r_2} \tag{5}$$

The mole fraction of polymer 1 radicals of type 1 is given by:

$$\phi_1 = \frac{k_{p21}f_1}{k_{p21}f_1 + k_{p12}f_2} \qquad \phi_2 = 1 - \phi_1 \tag{6}$$

This assumes that the long chain approximation is valid.

The following pseudo kinetic rate constants are used in modelling.

Thermal initiation of monomer:

$$k_{th} = k_{th1} f_1^3 + k_{th2} f_2^3 \quad (7)$$

Propagation:

$$k_p = k_{p11}\phi_1 f_1 + k_{p21}\phi_2 f_1 + k_{p12}\phi_1 f_2 + k_{p22}\phi_2 f_2 \quad (8)$$

Transfer to monomer:

$$k_{fm} = k_{fm11}\phi_1 f_1 + k_{fm21}\phi_2 f_1 + k_{fm12}\phi_1 f_2 + k_{fm22}\phi_2 f_2 \quad (9)$$

Transfer to chain transfer agent (or solvent):

$$k_{fts} = k_{fts1}\phi_1 + k_{fts2}\phi_2 \quad (10)$$

Termination by disproportionation:

$$k_{td} = k_{td11}\phi_1\phi_1 + 2k_{td12}\phi_1\phi_2 + k_{td22}\phi_2\phi_2 \quad (11)$$

Termination by combination:

$$k_{tc} = k_{tc11}\phi_1\phi_1 + 2k_{tc12}\phi_1\phi_2 + k_{tc22}\phi_2\phi_2 \quad (12)$$

Overall bimolecular termination rate constant:

$$k_t = k_{tc} + k_{td} \quad (13)$$

Decomposition reactions for monomer and polymer:

$$k_{dcm} = k_{dcm1} f_1 + k_{dcm2} f_2 \quad (14)$$

$$k_{dcp} = k_{dcp}\bar{F}_1 + k_{dcp2}\bar{F}_2 \quad (15)$$

Transfer to polymer:

$$k_{fp} = k_{fp11}\bar{F}_1\phi_1 + k_{fp21}\bar{F}_1\phi_2 + k_{fp12}\bar{F}_2\phi_1 + k_{fp22}\bar{F}_2\phi_2 \quad (16)$$

β-scission of terminal radicals:

$$k_\beta = k_{\beta 1}\phi_1 + k_{\beta 2}\phi_2 \quad (17)$$

β-scission of internal radicals:

$$k'_\beta = k'_{\beta 1}\bar{F}_1 + k'_{\beta 2}\bar{F}_2 \quad (18)$$

Backbiting:

$$k_b = k_{b11}\phi_1 F_1 + k_{b12}\phi_1 F_2 + k_{b21}\phi_2 F_1 + k_{b22}\phi_2 F_2 \quad (19)$$

Notice that, for backbiting, the instantaneous copolymer composition is used.

It should be noted that the use of pseudo kinetic rate constants for reactions including polymer is not strictly correct, since the composition of the chains will vary with monomer conversion. The use of $\bar{F}_1$ is an attempt to correct for compositional drift; however, for large extents of compositional drift, the errors introduced are uncertain. Since, in our case, the conversion is relatively low, and the comonomer composition is small, the composition drift is virtually insignificant (especially for ethylene–vinyl acetate[3] where $r_1 \simeq r_2 \simeq 1$). The use of pseudo kinetic rate constants should be a valid approximation for the branching reactions while being exact for the remaining propagation, termination and transfer reactions[49].

Mass balances on species

In order to find the rate of polymerization we must perform a mass balance on initiator species i:

$$d[I_i]/dL = -A_c k_{di}[I_i] \quad (\text{mol s}^{-1}\,\text{cm}^{-1}) \quad (20)$$

$$A_c = \pi r_i^2$$

and the rate of radical formation from initiator will be:

$$(RI)_{\text{initiator}} = \sum_i (n_i f_i k_{di}[I_i]) \quad (21)$$

where n_i is the number of radicals produced by one initiator molecule decomposing (usually $n_i = 2$), and f_i is the initiator efficiency.

The rate of radical production by thermal initiation of the monomer is:

$$(RI)_{\text{thermal}} = k_{th}[M]^3 \quad (22)$$

For polyethylene production, the thermal initiation of the monomer may not be important, since initiation rates by peroxides are usually much larger. However, it is included in order to provide analysis on runaway synthesis conditions in the reactor. The form of the rate expression for thermal initiation is from Buback[6], who studied the thermal polymerization of pure ethylene. He found that the activation energy for this reaction was quite large, about 53 kcal mol^{-1}, and therefore this reaction may not become significant (if at all) until high temperatures. The contribution of the comonomer to thermal initiation is not known.

Oxygen can both initiate and inhibit free-radical polymerization. Thus, the mass balances for O_2 and RO_2 are:

$$d[O_2]/dL = -A_c(k_{dO_2}[O_2][M] + k_r[O_2]Y_0) \quad (\text{mol s}^{-1}\,\text{cm}^{-1}) \quad (23)$$

$$d[RO_2]/dL = A_c(k_r[O_2]Y_0 - k_{dp}[RO_2]) \quad (\text{mol s}^{-1}\,\text{cm}^{-1}) \quad (24)$$

and the net rate of initiation by oxygen and decomposing peroxides formed from oxygen will be:

$$(RI)_{\text{oxygen}} = 2k_{dO_2}[O_2][M] + 2k_{dp}[RO_2] \quad (25)$$

where [M] is the total monomer concentration and $[RO_2]$ is the concentration of peroxides that form from the inhibition reaction by oxygen. Y_0 is the total radical concentration or equivalently the zeroth moment of the polymer radical distribution. The total rate of initiation will be given by

$$(RI)_{\text{initiator}} + (RI)_{\text{thermal}} + (RI)_{\text{oxygen}} \quad (26)$$

The rate of monomer consumption, for each monomer type (assuming long chain approximation), is given by:

$$d[M_i]/dL = -A_c(k_{pii}\phi_i Y_0[M_i] + k_{pji}\phi_i Y_0[M_i]) \quad (\text{mol s}^{-1}\,\text{cm}^{-1}) \quad (27)$$

The moles of monomer 1 and 2 bound as polymer can be calculated as

$$d\Psi_i/dL = A_c(k_{pii}\phi_i Y_0[M_i] + k_{pji}\phi_j Y_0[M_i] - k_{dcpi}\Psi_i) \quad (\text{mol s}^{-1}\,\text{cm}^{-1}) \quad (28)$$

We also need a balance on the moles of chain transfer agent (modifier or solvent) in the reactor:

$$d[TS]/dL = -A_c k_{fts}[TS]Y_0 \quad (29)$$

Heat transfer equations

The temperature profile along the reactor is an important calculation. The rate of polymerization can double for every 10°C rise in temperature, and thus, if the temperature profile is incorrect, the other predictions will certainly be inaccurate. We must also calculate the temperature profile for safety considerations. The energy

balance on the reactor contents, considering heat flow from the jacket to the reactor, results in:

$$\frac{dT}{dL} = \left(\frac{\overline{\Delta H}}{WC_p}\right)\left(\frac{d\Psi_1}{dL} + \frac{d\Psi_2}{dL}\right) + \left(\frac{U2\pi r_i}{WC_p}\right)(T_j - T) \quad (30)$$

where C_p is heat capacity of reaction mixture; $\overline{\Delta H}$ is average heat of polymerization (energy released per mole of monomer reacted), defined, for convenience, as a positive number; r_i is radius of reactor; T is reactor temperature at length L; T_j is jacket temperature at length L; L is length along the reactor; U is overall heat transfer coefficient; and W is mass flow of reaction mixture along the reactor.

The overall heat transfer coefficient U can be calculated by:

$$1/U = 1/h_i + 1/h_w$$

where h_i is heat transfer coefficient for film between reactor contents and reactor wall; and h_w is heat transfer coefficient from the jacket contents and through the jacket wall. This quantity must be either measured or estimated from the heat transfer data, for each heating/cooling zone. The first term is the resistance to heat transfer from the film inside the reactor; the second term is the resistance to heat transfer from the water/steam mixture to the film inside the reactor.

We can use the approach taken by Chen *et al.*[8], where the heat transfer coefficient for the wall is set to a constant for each heating/cooling zone. The thermal conductivity of polyethylene reaction mixture (cal cm^{-1} s^{-1} K^{-1}) is given by Eiermann *et al.*[13]) as:

$$K = \frac{5.0 \times 10^{-4} W_m + 3.5 \times 10^{-4} W_p}{W_m + W_p}$$

where W_m and W_p are masses of monomer and polymer (grams).

The viscosity of the monomer (poise) in the reactor is given by Carr *et al.*[7] as:

$$\eta_0 = 1.98 \times 10^{-4} + 1.15 \times 10^2/T^2 \qquad (T \text{ in } ^\circ C)$$

and the relative viscosity as:

$$\log_{10}(\eta_r) = 0.0313(Q_1)^{2/3}/(Q_0)^{1/2}$$

where

$$\eta_r = \frac{\text{solution viscosity}}{\text{solvent viscosity}}$$

and Q_0 and Q_1 are the zeroth and the first moments of the polymer molecular-weight distribution.

The solution viscosity (assuming that monomer is the solvent) is calculated by:

$$\eta_s = \eta_r \eta_0$$

The Reynolds number is:

$$Re = 2r_i \rho (V/A_c)/\eta_s$$

The Prandtl number is given by:

$$Pr = C_p \eta_s / K$$

The Nusselt number is given by:

$$Nu = 0.026 Re^{0.8} Pr^{0.33} \qquad Re > 10\,000$$

$$Nu = 0.166(Re^{2/3} - 125)Pr^{0.33}[1 + (2r_i/L)^{2/3}] \qquad Re < 10\,000$$

The inside heat transfer coefficient is given by:

$$h_i = KNu/2r_i$$

The heat capacity of the reaction mixture is assumed to be the sum of the heat capacities of the pure components and we are neglecting heats of mixing and solution.

REACTOR PRESSURE EFFECTS

The reactor pressure affects both the rates of reaction and the thermodynamic properties of the reaction mixture. The reactor pressure decreases along the reactor length to the pulse valve, where a larger pressure drop is experienced. Furthermore, the pulse valve is periodically opened and closed, to help reduce reactor fouling. All of these effects must be reasonably modelled.

Pressure profiles

Since the rate of reaction depends upon the reactor pressure, it is important that we adequately model the pressure profile down the reactor length. One method is to write a differential equation for the pressure drop for turbulent flow down a tube. This gives[10,29], from the definition of the fanning friction factor for turbulent flow:

$$dP/dL = -f_f \rho u^2 / g_c r_i \quad (31)$$

where f_f is the fanning friction factor, ρ is solution density, u is linear velocity, g_c is the gravitational constant used to convert kgm (kilograms mass) to kgf (kilograms force) and P is reactor pressure.

The fanning friction factor for turbulent flow, under these reactor conditions, is probably in the range[5]:

$$0.01 > f_f > 0.0791/Re^{1/4}$$

The solution of this equation should give a reasonable pressure profile down the reactor to the pulse valve. The total pressure drop should be of the order of 300 to 500 kgf cm^{-2}.

Pulse valve effects

In this section we are interested in the effect of the valve pulsing and thus varying the reactor pressure range and the reaction mixture flow rate. This pulsing causes the reaction mixture to heat up and cool down, owing to the change in: (a) reaction rates as the pressure changes; (b) flow rates causing variation in residence times; (c) heat transfer coefficients as the velocity changes; and (d) heat transfer coefficients as the fouling is allowed to accumulate, or is removed from the reactor wall. This pulse valve may also cause axial mixing, but, for the reasons discussed previously, we are neglecting this. We are also modelling this as a steady-state flow reactor, even though the reaction mixture is slightly increasing and decreasing in linear velocity. The optimum case would be to model unsteady flow, accounting for axial mixing. Unfortunately, this would involve solving a set of partial differential equations (in time and reactor length), and we may find that the approximations we have made here give a simpler, but nonetheless adequate, model.

Reactor fouling has not been studied for this type of reactor. Since we have no theoretical basis to model the fouling of the tubular reactor, we have neglected this. Furthermore Donati *et al.*[10] found in a pilot-scale reactor that the sinusoidal pulsing of the reactor had no

significant effect on mixing, heat transfer coefficient and pressure reduction, probably due to the low frequency (2 to 10 s per pulse) of pulsation, as compared to the much higher frequencies of turbulent motion (approximately 10^3 times greater). A large amount of axial mixing (denoted by a small Peclet number) over a significant length of reactor would be required to strip a reactor of any polymer film fouling the walls. Agrawal and Han[2] found that a Peclet number near 100 is needed for significant axial mixing. On the other hand Chen *et al.*[8] found that the Peclet number is more probably in the order of 10^{14} for a tubular reactor. For these reasons, we feel that we are still justified in neglecting axial mixing, and in neglecting any fouling on the reactor walls, because the axial mixing that would be present, due to the pulse valve, is not sufficient to strip the walls of any fouling.

Under usual operation, the pulse valve is quickly opened every T_{pulse} seconds, allowing a decrease in reactor entry pressure of ΔP (kgf cm^{-2}), and slowly closed over T_{close} seconds until the pressure returns to the set point. We assume that the valve is instantaneously opened and linearly closed with time. Since we have not yet developed any realistic model on how the pressure and mass flow rates change with valve position, we assume that the flow increases linearly, and the pressure decreases linearly with valve position as it is opened. The pressure change is a process variable, controlled by the operator, and the flow rate change may be of the order of 20 to 50% (Donati *et al.*[10]). We also assume that the pressure reduction due to the pulse valve, ΔP, is the same over the entire length of the reactor (up to the pulse valve). Thus the pressure profile down the reactor, P_0, is calculated as in the previous section, and periodic perturbations due to pulsing are superimposed upon this profile. A representation of the pressure profile is shown in *Figure 4*.

Pressure drop across the pulse valve

The pulse valve causes a large pressure drop from the reactor to the product cooler sections. This pressure drop can change the rate of any residual reactions and the temperature of the reaction mixture. The pressure drop is probably best modelled, in the absence of actual pressure data, as a constant value. This would appear as a discontinuity in the pressure profile down the reactor.

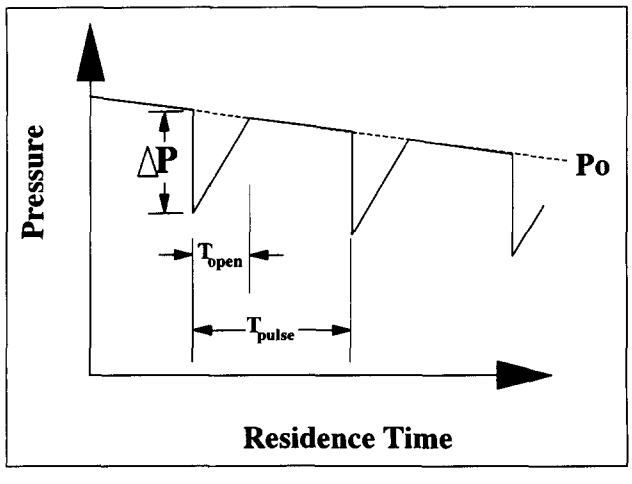

Figure 4 Description of effect of pulse valve on reactor pressure profile

The effect of the pulse valve can be considered to be a throttling phenomenon. This is a pressure drop at constant enthalpy, assuming that the heat losses to the surroundings are negligible. This is more familiarly known as Joule–Thomson expansion (for example see Smith and Van Ness[42]). The Joule–Thomson coefficient η_{JT} is defined as:

$$\eta_{JT} = (\partial T/\partial P)_H \tag{32}$$

This coefficient is a function of temperature, pressure and solution composition. In the absence of thermodynamic data, for the mixture under these conditions, we must assume that it is a constant and gives:

$$\eta_{JT} = (T_2 - T_1)/(P_2 - P_1) \tag{33}$$

So, given the pressure drop and the expansion coefficient, one can estimate the temperature change over the pulse valve. The coefficient η_{JT} is probably also a function of the valve type and fluid properties.

All the equations derived so far do not account for the microstructure of the resin produced. In order to make predictions on polymer properties, a knowledge of the molecular-weight averages and branching frequencies is of paramount importance, and these topics will be treated in the next sections.

MOLECULAR-WEIGHT CONSIDERATIONS

A precise knowledge of polymer properties is of great importance, as more and more specialties are required for specific industrial applications. In order to predict the physical properties of a resin, it is indispensable to know the molecular properties of the polymer. For this reason, molecular properties such as molecular-weight distribution and branching frequencies are very meaningful calculations for the model. From the industrial point of view, a reliable copolymerization model is capable of appraising synthesis conditions, as well as allowing studies on new copolymers prior to industrial tests. Thus, new polymer grades could be developed more easily, and the existing ones may be optimized in order to supply consistently high-quality resins to customers.

Several attempts to model the molecular weight and branching frequencies have been made (see following text and Appendix 3). In addition to the necessary initiation, propagation and termination reactions, some have included transfer to polymer and backbiting, but others have neglected either or both termination by combination and β-scission. Additionally, other authors only consider the β-scission of terminal radicals. The β-scission of internal radicals should also cleave long chains into two smaller macromolecules, thus preferentially reducing the molecular weight of the longer chains and narrowing the distribution. It has been observed[9] that, at temperatures above 210°C, molten polyethylene may tend to crosslink, while at temperatures above 290°C, chain scission may dominate. *Figures 5* and *6* (Hamielec *et al.*[21]) show the melt flow index (*MFI*) as a function of peroxide concentration for the degradation of polyethylene in an extruder or manual rheometer. In these processes, polyethylene is heated in the presence of a peroxide initiator. The initiator decomposes and abstracts a hydrogen from the polymer chain backbone. This internal radical can only undergo termination or β-scission since propagation is impossible owing to the absence of monomer. Termination by disproportionation

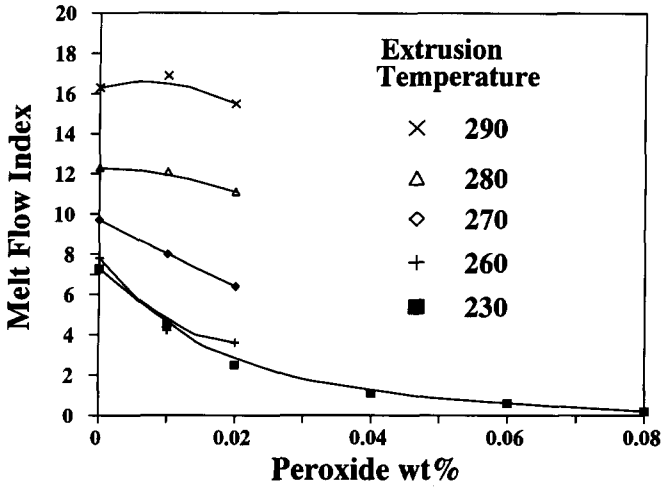

Figure 5 Simultaneous degradation and crosslinking of LLDPE initiated by peroxides during extrusion. *MFI* measured at 230°C and 10 kgf (Hamielec *et al.*[21])

will not affect the molecular weight and thus the melt flow index. Termination by combination will cause the molecular weight to increase (leading to a lower melt flow index), and β-scission will decrease the molecular weight (raising the value of melt flow index). We observe that, at lower temperatures (230°C), the *MFI* decreases with peroxide concentration, indicating that termination by combination is occurring to increase the molecular weight. At higher temperatures (280–290°C), the *MFI* tends to increase, at least at lower initiator concentrations, indicating the effect of the β-scission reaction, thus decreasing the molecular weight. Higher initiator concentrations tend to promote gelation (Hamielec *et al.*[21]).

From these data one can see that both termination by combination and β-scission are important in the melt, and we can only surmise that they are important under synthesis conditions as well.

With respect to high-pressure polyethylene reactors, a brief discussion of some of the past molecular-weight modelling attempts (only for homopolymerization) is in order.

Saidel and Katz[28,38] considered transfer to solvent and termination by combination and disproportionation but neglected the β-scission, transfer to polymer and backbiting reactions. They then used the method of moments to derive equations for the number- and weight-average molecular weights. They found that the moment equations were not closed, i.e. the lower moments were functions of the higher moments. In order to close the equations, a technique presented by Hulburt and Katz[26] was used. This technique assumes that the molecular-weight distribution can be represented as a truncated (after the first term) series of Laguerre polynomials by using a gamma distribution weighting function chosen so that the coefficients of the second and third terms are zero. It should be noted that this is still an empirical correlation for the higher moments as a function of the lower ones. This correlation may not be valid for many cases and quite possibly not for the polymer produced in this process (see Appendix 2).

Mullikin and Mortimer[34,35] used a probabilistic approach to find the instantaneous molecular-weight averages, including long chain branching, but excluding termination by combination, backbiting and β-scission. Small[40,41] used the same kinetic scheme as Mullikin and Mortimer and the method of generating functions to find the molecular-weight averages and the moments of the branching distribution. Jackson, Small and Whiteley[27] considered transfer to chain transfer agent, termination by disproportionation, termination by combination and transfer to polymer, but neglected backbiting and β-scission.

Agrawal and Han[2] included termination by combination, transfer to polymer, transfer to monomer and transfer to modifier but neglected backbiting and β-scission. Chen *et al.*[8] used the method of moments and the closure technique of Hulburt and Katz. The reaction scheme included termination by combination, transfer to polymer and β-scission of terminal radicals. Han and Liu[22] used this same kinetic mechanism.

Lee and Marano[31] used rate constants from Szabo *et al.*[44] and Ehrlich and Mortimer[11] and included transfer to monomer and modifier. Termination was by disproportionation and combination, and backbiting and transfer to polymer to produce branches were also included. The β-scission reaction was modelled for the break-up of the chains at tertiary carbon atoms in the backbone, and the β-scission rate constant would apparently include the fraction of radicals that are on tertiary carbon atoms. In actual fact, they neglected β-scission because they claim that most of the chains are made by either termination or transfer to modifier and because of uncertainty in the rate constant for the β-scission reaction.

Yamamoto and Sugimoto[51] used the model of Mullikin and Mortimer to estimate the long chain branching rate constant from their polymerization data. They included β-scission of terminal radicals and neglected termination by combination.

The model of Goto *et al.*[17] is based upon the probabilistic model suggested by Mullikin and Mortimer but they included the backbiting reaction to produce short chain branches as well as transfer to solvents, monomers and β-scission. Hollar and Ehrlich[25] added thermal initiation to the model of Chen *et al.*[8]. Kiparissides and Mavridis[29,33] included termination by combination and disproportionation, transfer to monomer, polymer and solvent, and β-scission of terminal radicals but neglected backbiting. They then used the method of

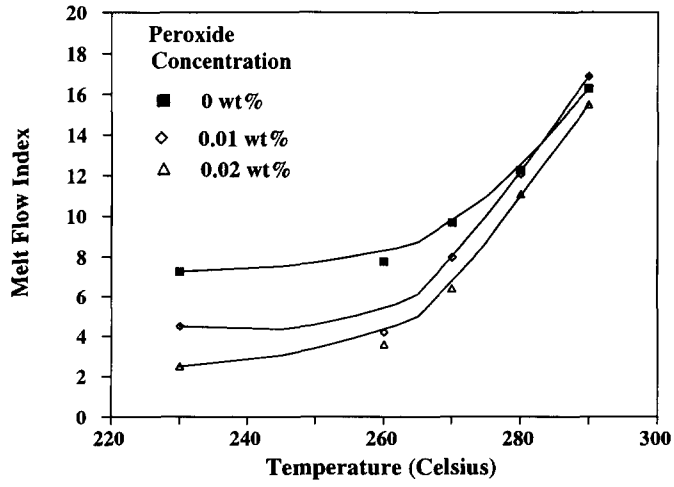

Figure 6 The effect of extrusion temperature and peroxide concentration on the simultaneous degradation and crosslinking of LLDPE (Hamielec *et al.*[21])

moments to find the number- and weight-average molecular weights, using the Hulburt and Katz[26] closure method when the stationary-state hypothesis was not used for the radical concentration. Gupta[18,19] used the same kinetics as Goto[17].

Yoon and Rhee[52] included only transfer to monomer, transfer to polymer and termination by combination. Shirodkar and Tsien[39] considered transfer to monomer, solvent and polymer, backbiting and termination by both combination and disproportionation, but neglected β-scission. Postelnicescu and Dumitrescu[37] considered termination by combination and disproportionation, transfer to monomer and transfer to chain transfer agent, but neglected transfer to polymer, backbiting and β-scission. Tjahjadi *et al.*[48] considered only termination by combination, neglecting all other reactions. Brandolin *et al.*[5] included termination by combination, transfer to polymer and solvent, and β-scission of terminal radicals.

What follows is our attempt to model the molecular weight and branching development for a more comprehensive set of reactions, including binary copolymerization. First, balances for the radicals and polymer chains of length r are given and then the method of moments is used to find the molecular-weight averages and the branching frequencies. The derivation of the molecular-weight moments, using this method, is as follows. Notice that we have used pseudo rate constants to convert the copolymerization equations into simpler homopolymer equations.

Moments of the molecular-weight distribution

For such a complex system, it is not possible without excessive computational effort to predict the entire molecular-weight distribution. The method of moments affords a relatively simple method to calculate the important averages. The moments of the molecular-weight distribution are found by writing balances on the radical and polymer molecules of chain length r, multiplying each term by the appropriate power of r and summing them from $r = 0$ to ∞.

The moments of the polymer radical size distribution are defined by:

$$Y_i = \sum_{r=1}^{\infty} r^i[\mathrm{R}(r)] \tag{34}$$

and the moments of the polymer size distribution are defined by:

$$Q_i = \sum_{r=2}^{\infty} r^i[\mathrm{P}(r)] \tag{35}$$

Radical moments

The radical centres can be either at the chain end or on the backbone of the chain (internal radicals). We assume that all internal radicals promptly undergo either propagation (forming long or short chain branches) or β-scission, i.e. the transfer to polymer reaction responsible for the production of the internal radical is the rate-limiting step. This is equivalent to assuming that the concentration of backbone radicals is near zero. We therefore neglect tetrafunctional branching and the possibility of crosslinking due to termination by combination of internal radicals.

Polymer radical moments

First, we must write a balance on radicals of unit length:

$$\begin{aligned}\frac{1}{A_c}\frac{\mathrm{d}[\mathrm{R}(1)]}{\mathrm{d}L} &= (RI) - k_r[\mathrm{R}(1)][\mathrm{O}_2] - k_p[\mathrm{R}(1)][\mathrm{M}] \\ &\quad - (k_{tc} + k_{td})Y_0[\mathrm{R}(1)] \\ &\quad + (\tau + k_\beta)\{Y_0 - [\mathrm{R}(1)]\} \\ &\quad - K_{LCB}[\mathrm{R}(1)]Q_1 - K_\beta[\mathrm{R}(1)]Q_1 \end{aligned} \tag{36}$$

where

$$\tau = k_{fm}[\mathrm{M}] + k_{fts}[\mathrm{TS}]$$

Then for length r ($r \geqslant 2$):

$$\begin{aligned}\frac{1}{A_c}\frac{\mathrm{d}[\mathrm{R}(r)]}{\mathrm{d}L} &= k_p[\mathrm{M}][\mathrm{R}(r-1)] - k_p[\mathrm{M}][\mathrm{R}(r)] \\ &\quad - (k_{tc} + k_{td})[\mathrm{R}(r)]Y_0 - (\tau + k_\beta)[\mathrm{R}(r)] \\ &\quad - K_{LCB}[\mathrm{R}(r)]Q_1 + K_{LCB}Y_0 r[\mathrm{P}(r)] \\ &\quad - K_\beta[\mathrm{R}(r)]Q_1 + K_\beta Y_0 \sum_{s=r+1}^{\infty}[\mathrm{P}(s)] \\ &\quad - k_r[\mathrm{R}(r)][\mathrm{O}_2] \end{aligned} \tag{37}$$

The radical moment equations are represented by:

$$\frac{\mathrm{d}Y_i}{\mathrm{d}L} = \frac{\mathrm{d}[\mathrm{R}(1)]}{\mathrm{d}L} + \sum_{r=2}^{\infty} r^i \frac{\mathrm{d}[\mathrm{R}(r)]}{\mathrm{d}L} \tag{38}$$

After substitution of radical balances in the expression above, and noting that:

$$Q_i \gg Q_{i-1} \gg Q_{i-2} \cdots$$
$$Y_i \gg Y_{i-1} \gg Y_{i-2} \cdots$$
$$Q_i \gg Y_i$$

we obtain:

$$\frac{1}{A_c}\frac{\mathrm{d}Y_0}{\mathrm{d}L} = (RI) - k_r Y_0[\mathrm{O}_2] - (k_{tc} + k_{td})Y_0^2 \tag{39}$$

$$\begin{aligned}\frac{1}{A_c}\frac{\mathrm{d}Y_1}{\mathrm{d}L} &= (RI) - k_r Y_1[\mathrm{O}_2] - (k_{tc} + k_{td})Y_1 Y_0 \\ &\quad + k_p[\mathrm{M}]Y_0 - (\tau + k_\beta)Y_1 \\ &\quad + K_{LCB}(Y_0 Q_2 - Y_1 Q_1) \\ &\quad + \tfrac{1}{2}K_\beta Y_0 Q_2 - K_\beta Q_1 Y_1 \end{aligned} \tag{40}$$

$$\begin{aligned}\frac{1}{A_c}\frac{\mathrm{d}Y_2}{\mathrm{d}L} &= (RI) - k_r Y_2[\mathrm{O}_2] - (k_{tc} + k_{td})Y_2 Y_0 \\ &\quad + 2k_p[\mathrm{M}]Y_1 - (\tau + k_\beta)Y_2 \\ &\quad + K_{LCB}(Y_0 Q_3 - Y_2 Q_1) \\ &\quad + \tfrac{1}{3}K_\beta Y_0 Q_3 - K_\beta Q_1 Y_2 \end{aligned} \tag{41}$$

$$\begin{aligned}\frac{1}{A_c}\frac{\mathrm{d}Y_3}{\mathrm{d}L} &= (RI) - k_r Y_3[\mathrm{O}_2] - (k_{tc} + k_{td})Y_3 Y_0 \\ &\quad + 3k_p[\mathrm{M}]Y_2 - (\tau + k_\beta)Y_3 \\ &\quad + K_{LCB}(Y_0 Q_4 - Y_3 Q_1) \\ &\quad + \tfrac{1}{4}K_\beta Y_0 Q_4 - K_\beta Q_1 Y_3 \end{aligned} \tag{42}$$

Stationary-state hypothesis. The stationary-state hypothesis (s.s.h.) for the radical moments is used. Mavridis

and Kiparissides[29,33] and Yoon and Rhee[52] found little difference in the solution to the *MWD* when the s.s.h. assumption is relaxed. Moreover, in our simulations, when the s.s.h. was relaxed the results were not significantly changed. The assumption makes the o.d.e.'s much easier to solve, as they become less stiff. Using the s.s.h., the radical concentrations are given by the following simple expressions:

$$Y_0 = \frac{\{(k_r[O_2])^2 + 4(k_{tc} + k_{td})(RI)\}^{1/2} - k_r[O_2]}{2(k_{tc} + k_{td})} \quad (43)$$

$$Y_1 = \frac{(RI) + k_p[M]Y_0 + K_{LCB}Y_0Q_2 + \frac{1}{2}K_\beta Y_0Q_2}{k_r[O_2] + (k_{tc} + k_{td})Y_0 + (\tau + k_\beta) + K_{LCB}Q_1 + K_\beta Q_1} \quad (44)$$

$$Y_2 = \frac{(RI) + 2k_p[M]Y_1 + K_{LCB}Y_0Q_3 + \frac{1}{3}K_\beta Y_0Q_3}{k_r[O_2] + (k_{tc} + k_{td})Y_0 + (\tau + k_\beta) + K_{LCB}Q_1 + K_\beta Q_1} \quad (45)$$

$$Y_3 = \frac{(RI) + 3k_p[M]Y_2 + K_{LCB}Y_0Q_4 + \frac{1}{4}K_\beta Y_0Q_4}{k_r[O_2] + (k_{tc} + k_{td})Y_0 + (\tau + k_\beta) + K_{LCB}Q_1 + K_\beta Q_1} \quad (46)$$

Polymer moments. A balance on polymer chains of length r gives:

$$\begin{aligned}\frac{1}{A_c}\frac{d[P(r)]}{dL} = {} & k_{td}[R(r)]Y_0 + \tfrac{1}{2}k_{tc}\sum_{s=1}^{r-1}[R(r-s)][R(s)] \\ & + k_r[O_2][R(r)] + K_{LCB}[R(r)]Q_1 \\ & - K_{LCB}Y_0r[P(r)] \\ & + (\tau + k_\beta)[R(r)] - K_\beta Y_0r[P(r)] \\ & + K_\beta Y_0\sum_{s=r+1}^{\infty}[P(s)] \\ & + K_\beta Q_1[R(r)] \end{aligned} \quad (47)$$

Multiplying this equation by the appropriate power of r and then summing, we get the following moments of the polymer size distribution:

$$\begin{aligned}\frac{1}{A_c}\frac{dQ_0}{dL} = {} & k_{td}Y_0^2 + \tfrac{1}{2}k_{tc}Y_0^2 + k_r[O_2]Y_0 \\ & + (\tau + k_\beta)Y_0 + K_\beta Y_0Q_1 \end{aligned} \quad (48)$$

$$\begin{aligned}\frac{1}{A_c}\frac{dQ_1}{dL} = {} & k_{td}Y_0Y_1 + k_{tc}Y_1Y_0 + k_r[O_2]Y_1 + (\tau + k_\beta)Y_1 \\ & + K_{LCB}(Q_1Y_1 - Y_0Q_2) + K_\beta Q_1Y_1 - \tfrac{1}{2}K_\beta Y_0Q_2 \\ \simeq {} & k_p[M]Y_0 \end{aligned} \quad (49)$$

Table 1 Actual molecular-weight data for low-density polyethylene from a tubular reactor at Triunfo, Brazil

Resin	$\bar{M}_n$	$\bar{M}_w$	$\bar{M}_z$
Resin A	25 900	222 000	705 000
Resin B (sample 1)	15 800	88 300	273 000
Resin B (sample 2)	16 700	97 800	312 000
Resin C	21 300	148 000	445 000
Resin D	20 500	135 000	398 000
Resin E (sample 1)	17 800	95 800	307 000
Resin E (sample 2)	17 800	99 300	330 000
Resin E (sample 3)	18 900	98 500	284 000

using long chain approximation

$$\begin{aligned}\frac{1}{A_c}\frac{dQ_2}{dL} = {} & k_{td}Y_0Y_2 + k_{tc}(Y_0Y_2 + Y_1^2) \\ & + k_r[O_2]Y_2 + (\tau + k_\beta)Y_2 \\ & + K_{LCB}(Q_1Y_2 - Y_0Q_3) + K_\beta Q_1Y_2 - \tfrac{2}{3}K_\beta Y_0Q_3 \end{aligned} \quad (50)$$

$$\begin{aligned}\frac{1}{A_c}\frac{dQ_3}{dL} = {} & k_{td}Y_0Y_3 + k_{tc}(Y_0Y_3 + 3Y_1Y_2) \\ & + k_r[O_2]Y_3 + (\tau + k_\beta)Y_3 \\ & + K_{LCB}(Q_1Y_3 - Y_0Q_4) + K_\beta Q_1Y_3 - \tfrac{3}{4}K_\beta Y_0Q_4 \end{aligned} \quad (51)$$

The number- and weight-average chain lengths are given respectively by:

$$\bar{r}_n = (Q_1 + Y_1)/(Q_0 + Y_0) \simeq Q_1/Q_0 \quad (52)$$

$$\bar{r}_w = (Q_2 + Y_2)/(Q_1 + Y_1) \simeq Q_2/Q_1 \quad (53)$$

and the z-average chain length by:

$$\bar{r}_z = (Q_3 + Y_3)/(Q_2 + Y_2) \simeq Q_3/Q_2 \quad (54)$$

since $Q_i \gg Y_i$.

The problem of closure

As we can see, the internal radical β-scission terms in the moment equations of the molecular-weight distribution are functions of higher moments; therefore, the system is not 'closed' when this reaction is significant. Notice that the $K_{LCB}Y_0Q_4$ terms will cancel out upon substitution for Y_3, but the β-scission terms ($K_\beta Y_0Q_4$) will not. For this reason, we must arrive at a closure technique that will adequately predict the higher moments as a function of the lower ones. We have selected two possible choices for a closure technique as described below, and have evaluated each of them by simulation, and compared with actual measured molecular weights.

The method of Hulburt and Katz. Several authors have used the closure technique of Hulburt and Katz[26], although this method may not be completely suitable for polyethylene produced in a high-pressure tubular reactor (see Appendix 2). Nevertheless, this technique will be evaluated as a possible closure method. The closure equation is:

$$Q_3 = \frac{Q_2}{Q_1Q_0}(2Q_2Q_0 - Q_1^2) \quad (55)$$

Assuming a log-normal distribution. Molecular-weight distributions produced in tubular reactors tend to appear to be log-normal. For this reason, we shall assume that the distribution is log-normal, and derive expressions for the higher moments as a function of the lower moments (see Appendix 1 for the derivation), and the result is:

$$Q_3 = Q_0(Q_2/Q_1)^3 \quad (56)$$

Comparison with actual data

Some actual molecular-weight data for LDPE were provided by Poliolefinas, and are shown in *Table 1*.

If Q_0 is set to unity, one can calculate the higher moments from the molecular-weight data, since $\bar{M}_n = mQ_1/Q_0$, $\bar{M}_w = mQ_2/Q_1$ and $\bar{M}_z = mQ_3/Q_2$ (m is the

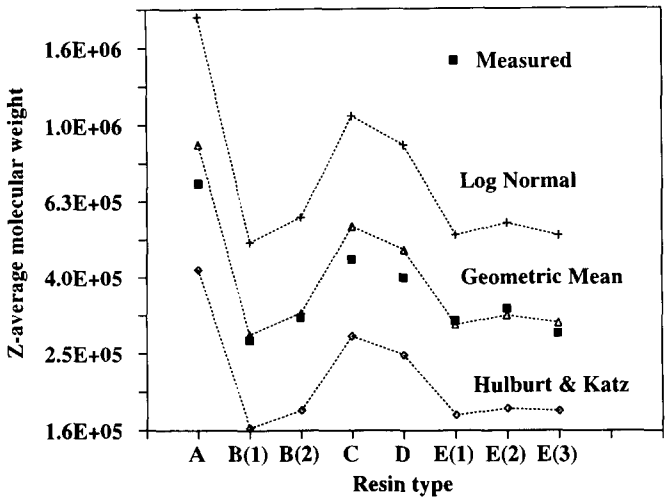

Figure 7 Correlating plant molecular-weight data with closure techniques (M_z data from tubular reactor)

molecular weight of monomer). One can therefore calculate the third moment (and thus M_z) as given by the Hulburt and Katz (HK) and log-normal (LN) methods and compare the results with those presented above. These are shown in *Figure 7*. We can see that the LN method greatly overpredicts the Q_3 value, whereas the HK method underpredicts it. The geometric average of the two methods is in good agreement with plant reactor data:

$$Q_{3,\text{geometric}} = (Q_{3,\text{HK}}Q_{3,\text{LN}})^{1/2}$$

Recommendations for closure

On the basis of these tests, the method of choice appears to be the geometric mean of the Hulburt and Katz method and the log-normal method. It should be emphasized that the method that fits the actual plant data best (in this case, the geometric mean) should be used for simulations. Closure methods should not be arbitrarily chosen without validation with real data.

OVERALL REACTION RATE CONSTANTS INVOLVING INTERNAL RADICALS

We have written the internal radical β-scission, long and short chain branching rates as overall reactions, even though they are two-step reactions, the first step being some sort of transfer to polymer (either by a radical attacking a polymer chain, or by backbiting), and the second step being either scission or propagation which forms branches. The internal radicals can also be consumed by transfer to monomer or to chain transfer agent and, although much less likely, by termination. Internal radicals are shielded by the coiled chain, and surrounded by monomer. For termination to occur, a growing macroradical must penetrate the coiled chain and approach the radical centre before the radical centre has a chance to propagate. With the large amount of monomer present, this seems to be a negligible reaction. It should be noted that this reaction is very important during polymer degradation in an extruder, where there is no monomer present and significant crosslinking can occur.

Let us consider two types of internal radicals, one formed by transfer to polymer by another radical, and one formed by backbiting, the former leading to a long chain branch and the latter to a short chain branch. A balance on these two types of internal radicals of chain length r gives the following. Long chain branch radicals:

$$\frac{1}{A_c}\frac{d[R'_L(r)]}{dL} = k_{fp}r[P(r)]Y_0 - (k_p[M] + k'_\beta + \tau)R'_L(r)] \quad (57)$$

Short chain branch radicals:

$$\frac{1}{A_c}\frac{d[R'_S(r)]}{dL} = k_b[R(r)] - (k_p[M] + k'_\beta + \tau)[R'_S(r)] \quad (58)$$

Making the stationary-state hypothesis for these internal radicals, expressions for the concentrations of these internal radicals follow:

$$[R'_L(r)] = \left(\frac{k_{fp}}{k_p[M] + k'_\beta + \tau}\right)r[P(r)]Y_0$$
$$[R'_S(r)] = \left(\frac{k_b}{k_p[M] + k'_\beta + \tau}\right)[R^*(r)] \quad (59)$$

and the total concentrations:

$$[R'_L] = \left(\frac{k_{fp}}{k_p[M] + k'_\beta + \tau}\right)Q_1Y_0$$
$$[R'_S] = \left(\frac{k_b}{k_p[M] + k'_\beta + \tau}\right)Y_0 \quad (60)$$

Considering the generation of long chain branches, we realize that:

$$\frac{1}{A_c}\frac{d(LCB)}{dL} = k_p[M][R'_L] = k_p[M]\left(\frac{k_{fp}}{k_p[M] + k'_\beta + \tau}\right)Q_1Y_0 = K_{LCB}Q_1Y_0 \quad (61)$$

and for short chain branches:

$$\frac{1}{A_c}\frac{d(SCB)}{dL} = k_p[M][R'_S] = k_p[M]\left(\frac{k_b}{k_p[M] + k'_\beta + \tau}\right)Y_0 = K_{SCB}Y_0 \quad (62)$$

where

$$K_{LCB} = k_p[M]\left(\frac{k_{fp}}{k'_\beta + k_p[M] + \tau}\right) \quad (63)$$

and

$$K_{SCB} = k_p[M]\left(\frac{k_b}{k'_\beta + k_p[M] + \tau}\right) \quad (64)$$

The rate of β-scission of internal radicals is given by:

$$\frac{1}{A_c}\frac{d\beta}{dL} = k'_\beta[R'_L] = k'_\beta\left(\frac{k_{fp}}{k'_\beta + k_p[M] + \tau}\right)Q_1Y_0 = K'_\beta Q_1Y_0 \quad (65)$$

where β is the moles of internal radicals undergoing β-scission per unit time (mol s^{-1}) and:

$$K_\beta = k'_\beta\left(\frac{k_{fp}}{k'_\beta + k_p[M] + \tau}\right) \quad (66)$$

This neglects the contribution to the internal radical concentration made by backbiting. Backbiting tends to give internal radical centres two or three units from the end of the chain, and not uniformly along the chain. This is quite possibly[11,36] the mechanism for β-scission of terminal radicals described above. Since we have already accounted for this effect, we shall neglect the contribution to the internal radicals produced by backbiting.

It is not clear whether the β-scission of internal radicals has an appreciable effect on the molecular weight during polyethylene synthesis. Under industrial conditions, transfer to modifier may produce many more *dead* polymer chains than does β-scission. Only comparison of the model predictions with industrial data can provide clarification of the importance of the β-scission reaction.

We have written all of these two-step reactions as overall reactions, with a sort of grouped rate constant for each overall reaction. One last note is that we have written these equations considering a homopolymer; for the copolymer case, pseudo rate constants should be adopted.

BRANCHING FREQUENCIES

The short and long chain branching can have an important effect on polymer properties. The more short chain branches incorporated along the polymer chain, the lower will be the polymer density, while long chain branches affect the rheological properties. The short chain branches are produced by the backbiting reaction; therefore, the number of short chain branches produced (SCB) is:

$$\frac{1}{A_c}\frac{d(SCB)}{dL} = K_{SCB}Y_0 \quad (67)$$

Long chain branches are produced by the transfer to polymer reaction. Thus, the total number of long chain branches produced (LCB) is given by:

$$\frac{1}{A_c}\frac{d(LCB)}{dL} = K_{LCB}Y_0Q_1 \quad (68)$$

The number of short and long chain branches per polymer molecule is calculated as follows:

$$\bar{S}_n = (SCB)/Q_0 \quad (69)$$

$$\bar{L}_n = (LCB)/Q_0 \quad (70)$$

The number of short and long chain branches per 1000 carbon atoms is given by (assuming two backbone carbon atoms per monomer unit):

$$\lambda_S = [(SCB)/Q_1] \times 500 \quad (71)$$

$$\lambda_L = [(LCB)/Q_1] \times 500 \quad (72)$$

The expressions derived above permit one to calculate the branching frequencies. Consequently, it will be possible to control some of the polymer physical properties (such as density) and rheological properties (such as melt flow) through variation in operating conditions of the reactor.

SOLUTION OF THE MATHEMATICAL MODEL

The model comprises a system of coupled ordinary differential equations. These equations may become stiff during the nearly adiabatic temperature rise. To solve these equations, we have used a package called LSODE[23,24] that uses either a non-stiff (Adams) or stiff (Gear) method with variable step size and interpolating polynomial order.

SIMULATIONS

Some typical conversion, temperature, molecular weight and branching frequency profiles are presented in *Figures 8, 9, 10* and *11*. These profiles were generated using the simulation program TUBULAR and are simply to show standard trends in a multiple-feed, multiple-reaction-zone tubular reactor. The inflow points of monomer, modifier and initiator are shown in these figures. Conversion is presented as the mass of polymer divided by the mass of monomer and polymer.

In order to evaluate the validity of the model developed, simulations for both homopolymerization and copolymerization were carried out to compare the

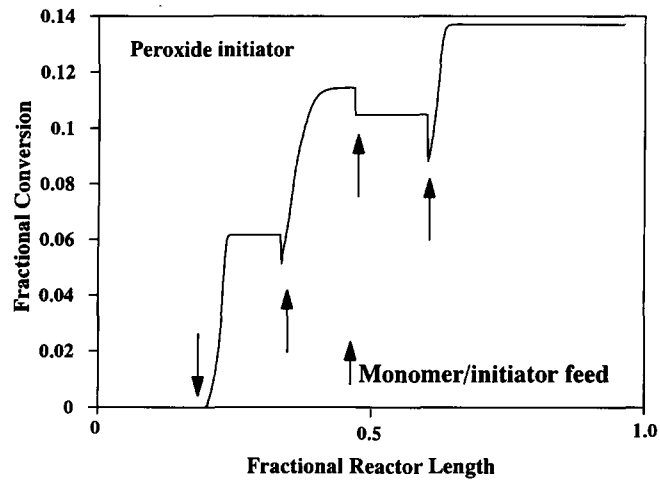

Figure 8 Typical conversion profile: peroxide initiated homopolymer

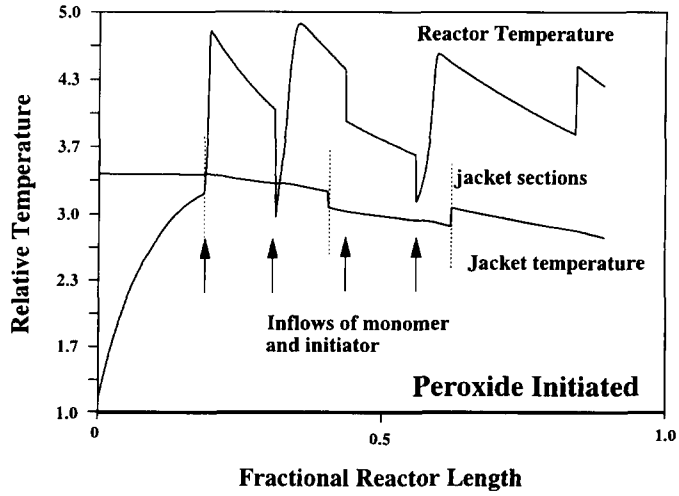

Figure 9 Typical reactor temperature profile: peroxide initiated homopolymer

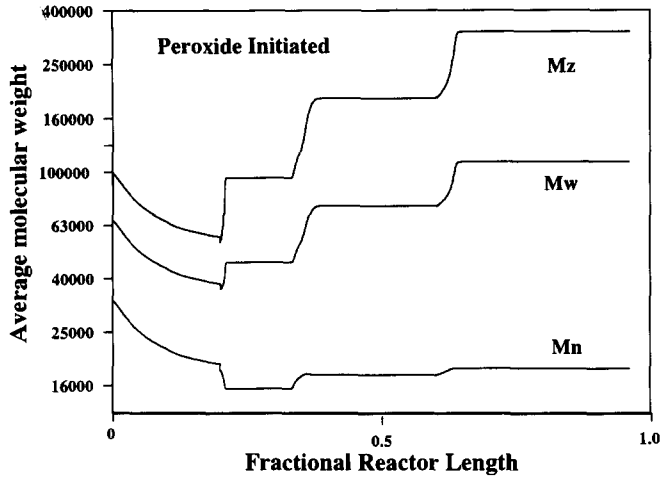

Figure 10 Typical molecular weight-average profile: peroxide initiated homopolymer

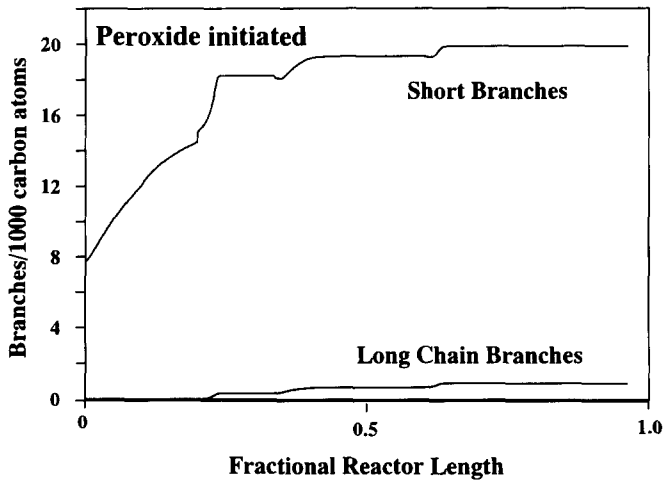

Figure 11 Typical branching frequency profile: peroxide initiated homopolymer

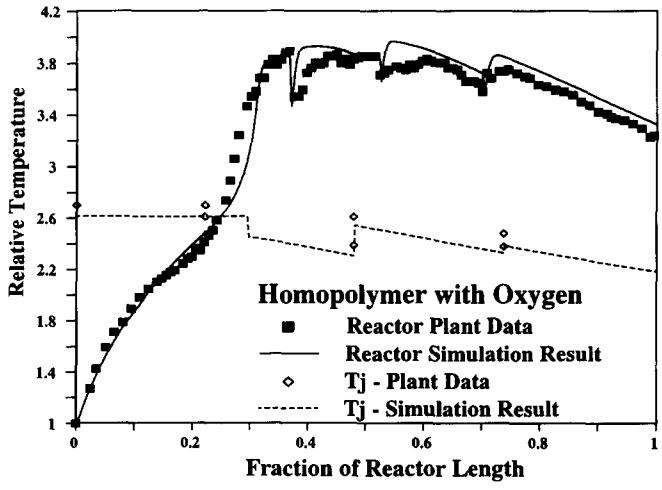

Figure 12 Temperature profile: oxygen initiated homopolymer

model predictions with actual plant data. Since the literature values of the kinetic rate constants seem to vary over a wide range[18], we chose to fit the parameters to industrial data. For this reason the values of the rate constants used must remain proprietary. The results are shown in figures below. *Figures 12* and *13* show the reactor and jacket temperature (T_j) profiles, as well as monomer conversion along the reactor for homopolymerization of ethylene using oxygen as initiator, while *Figures 14* and *15* employ liquid peroxides instead. *Figures 16* and *17* provide the same plots for copolymerization of ethylene and vinyl acetate. For copolymer, the conversion is the total conversion of monomer.

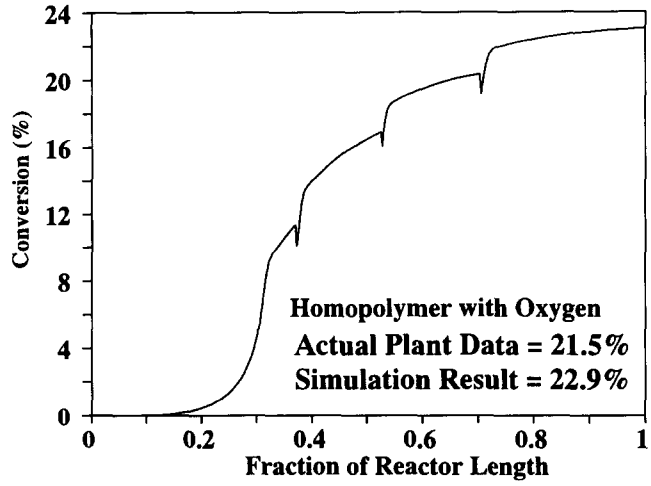

Figure 13 Conversion profile: oxygen initiated homopolymer

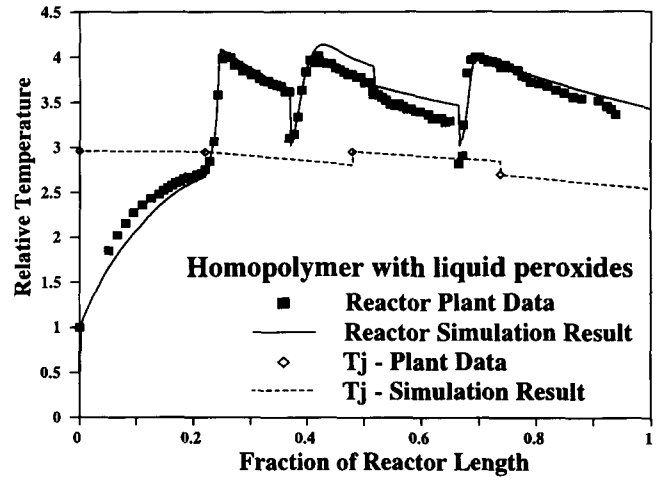

Figure 14 Reactor temperature profile: peroxide initiated homopolymer

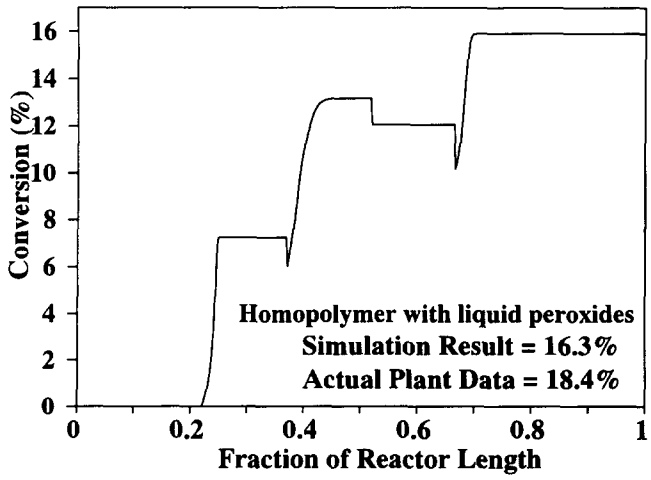

Figure 15 Conversion profile: peroxide initiated homopolymer

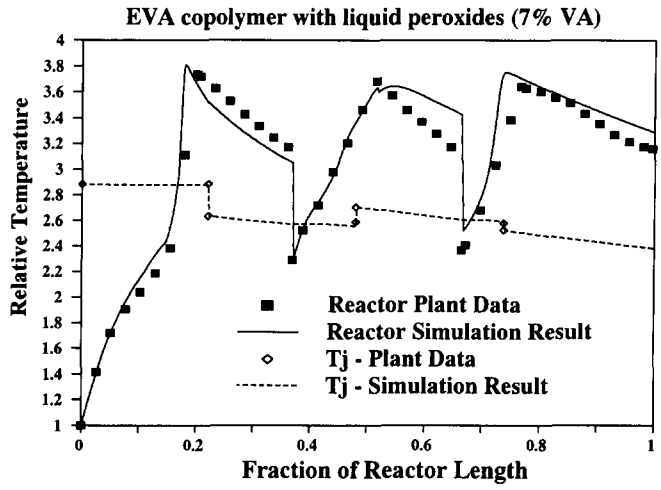

Figure 16 Reactor temperature profile: peroxide initiated copolymer

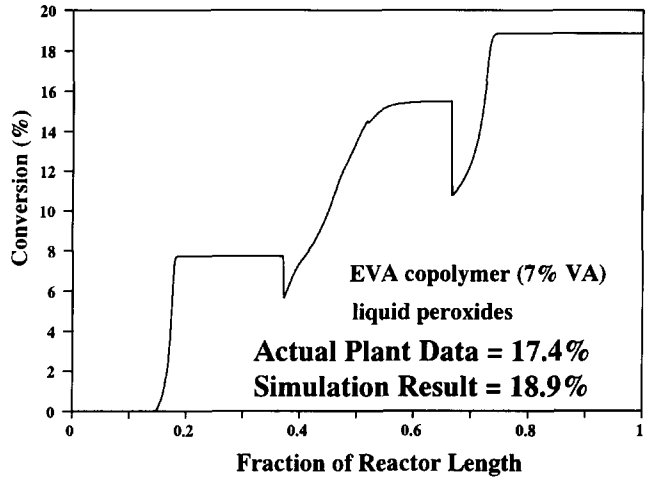

Figure 17 Conversion profile: peroxide initiated copolymer

Notice that, in all cases, the model predictions fit the plant data reasonably well, suggesting that the model proposed has the necessary structure and fundamental basis to simulate the industrial reactor. However, efforts still have to be made in the sense of improving parameter estimates of the model, with respect to the molecular properties, and work is currently being done in this direction by measuring molecular properties, and fitting the model parameters.

SUMMARY

A more general kinetic model has been developed for free-radical, high-pressure copolymerization in a commercial tubular-type reactor with multiple feeding points. The model accounts for reactions that are frequently neglected by other authors, like thermal initiation of monomer, backbiting, β-scission and decomposition reactions. In order to represent realistically the polymerization process, the effect of pulse valve and product cooler was also incorporated in the model. In order to have a better understanding of how reactor operation policies affect the polymer microstructure (and in turn the polymer properties), the model was extended to predict both the molecular-weight average and the average frequency of long and short chain branching. A new approach for moment closure to evaluate molecular-weight averages has also been presented. Simulation results generated from the model were compared with plant data, and have shown encouraging prospects for industrial application. More data collection and parameter estimation is under way.

NOMENCLATURE

Subscripts and superscripts

1, 2	pertain to monomer type 1 (and 2) or monomer type 1 (and 2) repeat units
S, L	pertain to short and long chain branches
$'$	denotes internal radical
$=$	denotes terminal double bond
$\overline{\ }$	denotes accumulated properties

General

A_c	cross-sectional area of tubular reactor of constant cylindrical cross section
C_p	heat capacity of reaction mixture
$\overline{\Delta H}$	average heat of polymerization
f	initiator efficiency
f_f	fanning friction factor
f_1	comonomer composition, the mole fraction of monomer 1
F_1	instantaneous copolymer composition, the instantaneous mole fraction of monomer type 1 units in the chain
$\bar{F}_1$	accumulated copolymer composition, the accumulated mole fraction of monomer type 1 units in the chain
g_c	gravitational constant used to convert kgm (kilograms mass) to kgf (kilograms force)
h_i	heat transfer coefficient for film between reactor contents and reactor wall
h_w	heat transfer coefficient from the jacket contents and through the jacket wall
k	rate constant in appropriate units for the order of reaction
L	axial coordinate of the reactor
(LCB)	the number of long chain branches in the reaction volume
$\bar{L}_n$	the number of long chain branches per polymer molecule
M_i	molar flow rate of monomer type i
m	molecular weight of monomer
n	the number of radicals formed per peroxide molecule
P	reactor pressure
$\bar{M}_n$	number-average molecular weight
$\bar{M}_w$	weight-average molecular weight
$\bar{M}_z$	z-average molecular weight
$\bar{r}_n$	number-average chain length
$\bar{r}_w$	weight-average chain length
$\bar{r}_z$	z-average chain length
$P(r)$	polymer molecule of chain length r
$P^*(r)$	polymer molecule of chain length r with a terminal double bond
Q_i	the ith moment of the polymer molecular-weight distribution
r_i	reactor radius
(RI)	rate of initiation
$R(r)$	radicals of chain length r
$R'(r)$	internal radical of length r
(SCB)	the number of short chain branches in the reaction volume

$\bar{S}_n$	the number of short chain branches per polymer molecule
t	time
T	reactor temperature at length L
T_j	jacket temperature at length L
u	linear velocity
U	overall heat transfer coefficient
V	volumetric flow rate of reaction mixture
W	mass flow rate of the reaction mixture
W_p, W_m	mass of polymer and monomer
[X]	concentration of any species X
Y_i	the ith moment of the total radical molecular-weight distribution

Greek letters

ϕ_1	fraction of radical centres that are on monomer type 1 units
ρ	solution density
η_{JT}	Joule–Thomson coefficient
η_0	monomer viscosity
η_r	relative viscosity
η_s	solution viscosity
Ψ_i	moles of monomer i bound as polymer
λ_L	the number of long chain branches per 1000 carbon atoms
λ_S	the number of short chain branches per 1000 carbon atoms
τ	a grouping of kinetic parameters and concentrations related to the transfer to small molecule reactions

Rate constants

k_b	backbiting reaction
k'_β	β-scission reaction of an internal radical
k_β	β-scission reaction of a terminal radical
k_d	initiator decomposition reaction
k_{db}	terminal double-bond reaction
k_{dcm}	decomposition of monomer reaction
k_{dcp}	decomposition of polymer reaction
k_{dO_2}	oxygen initiation reaction
k_{dp}	slow initiation reaction
k_{fm}	transfer to monomer reaction
k_{fp}	transfer to polymer reaction
k_{fts}	transfer to chain transfer agent reaction
K_β	overall β-scission reaction for internal radicals
K_{LCB}	overall long chain branches reaction
K_{SCB}	overall short chain branches reaction
k_{pji}	propagation reaction
k_r	inhibition reaction for oxygen
k_{tcji}	termination by combination reaction
k_{tdji}	termination by disproportionation reaction
k_{th}	thermal initiation reaction

ACKNOWLEDGEMENTS

The authors wish to express their gratitude to Poliolefinas SA for the financial support of this project, and permission to publish the results. Thanks are also due to Mr A. B. de Carvalho, for his careful consideration and constructive criticism of the model and software.

REFERENCES

1 Agrawal, S. C., Ph.D. Thesis, Polytechnic Institute of New York, Brooklyn, 1974
2 Agrawal, S. C. and Han, C. D. *AIChE J.* 1975, **21**(3), 449
3 Beasley, J. K. in 'Comprehensive Polymer Science' (Eds. G. Allen and J. C. Bevington), Pergamon Press, Oxford, 1989, Vol. 3, p. 273
4 Bird, R. B., Stewart, W. E. and Lightfoot, E. N. 'Transport Phenomena', Wiley, New York, 1960, p. 186
5 Brandolin, A., Capiati, N. J., Farber, J. N. and Valles, E. M. *Ind. Eng. Chem. Res.* 1988, **27**, 784
6 Buback, M. *Makromol. Chem.* 1980, **181**, 373
7 Carr, N. L., Parent, J. D. and Peck, R. E. *Chem. Eng. Prog. Symp. Ser.* 1955, **51**(6), 91
8 Chen, C. H., Vermeychuk, J. G., Howell, J. A. and Ehrlich, P. *AIChE J.* 1976, **22**(3), 463
9 Cogswell, F. N. 'Polymer Melt Rheology', Wiley, New York, 1981, p. 153
10 Donati, G., Marini, L., Marziano, G., Mazzateri, C., Sampitano, M. and Langianni, E., Proc. 7th Int. Symp. Chem. React. Eng., Boston, 1982, p. 579
11 Ehrlich, P. and Mortimer, G. A. *Adv. Polym. Sci.* 1970, **1**, 386
12 Ehrlich, P. and Pittilo, R. N. J. *Polym. Sci.* 1960, **43**, 389
13 Eiermann, K. *Modellmassige Deutung Warmeleitfahigkeit Hochpolym. K., Koll. Z.* 1965, **201**, 3
14 Fawcett, E. W., Gibson, R. O., Perrin, M. W., Paton, J. G. and Williams, E. G. Br. Pat. 471590, (ICI); *Chem. Abstr.* 1938, **32**, 13626
15 Foster, G. N., MacRury, T. B. and Hamielec, A. E. in 'Liquid Chromatography of Polymers and Related Materials II' (Eds. J. Cazes and X. Delamare), Marcel Dekker, New York, 1980
16 Gierth, V. V. *Angew. Makromol. Chem.* 1970, **12**, 9
17 Goto, S., Yamamoto, K., Furui, S. and Sugimoto, M. *J. Appl. Polym. Sci.* 1981, **36**, 21
18 Gupta, S. K. *Current Sci.* 1987, **56**, No. 19
19 Gupta, S. K., Kumar, A. and Krishnamurthy, M. V. G. *Polym. Sci. Eng.* 1985, **25**, No. 1
20 Hamielec, A. E. and MacGregor, J. F. in 'Polymer Reaction Engineering' (Eds. K. H. Reichert and W. Geiseler), Hanser Publishers, New York, 1983, p. 21
21 Hamielec, A. E., Gloor, P. E., Zhu, S. and Tang, Y. COMPALLOY '90, Proc. 2nd Int. Congr. on Compatibilizers, and Reactor Polymer Alloying, Schotland, New Orleans, 7–9 March, 1990
22 Han, C. D. and Liu, T.-J. *Kwahak Konghak* 1977, **15**(4), 249
23 Hindmarsh, A. C. *ACM-Signum Newslett.* 1980, **15**(4), 10
24 Hindmarsh, A. C. in 'Scientific Computing' (Eds. S. Stepleman *et al.*), North-Holland, Amsterdam, 1983, pp. 55–64 (Vol. 1 of *IMACS Trans. Sci. Comput.*)
25 Hollar, W. and Ehrlich, P. *Chem. Eng. Commun.* 1983, **24**, 57
26 Hulburt, H. M. and Katz, S. *Chem. Eng. Sci.* 1964, **19**, 555
27 Jackson, R. A., Small, P. A. and Whiteley, K. S. *J. Polym. Sci., Polym. Chem. Edn.* 1973, **11**, 1781
28 Katz, S. and Saidel, G. M. *AIChE J.* 1967, **13**(2), 319
29 Kiparissides, C. and Mavridis, H. in 'Chemical Reactor Design and Technology' (Ed. H. de Lasa), NATO ASI Ser. E: Appl. Sci., No. 110, 1985
30 Laurence, R. L. and Pottiger, M. T., Private communication with Tjahjadi *et al.*, 1985
31 Lee, K. H. and Marano, J. P. Jr *ACS Symp. Ser.* 1979, **104**, 221
32 Marano, J. P. in 'Polymer Reaction Engineering—An Intensive Short Course on Polymer Production Technology', School of Chemical Technology, University of New South Wales, Sydney, Australia, 1979, Section 3, p. 7
33 Mavridis, H. and Kiparissides, C. *Polym. Process. Eng.* 1985, **3**, 263
34 Mullikin, R. V. and Mortimer, G. A. *J. Macromol. Sci.–Chem. (A)* 1970, **4**(7), 1495
35 Mullikin, R. V. and Mortimer, G. A. *J. Macromol. Sci.–Chem. (A)* **6**(7), 1301
36 Nicolas, L. *J. Chim. Phys.* 1958, **55**, 177
37 Postelnicescu, P. and Dumitrescu, A. M. *Materiale Plastice* 1987, **24**, No. 2
38 Saidel, G. M. and Katz, S. *J. Polym. Sci. (A-2)* 1968, **6**, 1149
39 Shirodkar, P. P. and Tsien, G. O. *Chem. Eng. Sci.* 1986, **41**(4), 1031
40 Small, P. A. *Polymer* 1972, **13**, 536
41 Small, P. A. *Polymer* 1973, **14**, 524
42 Smith, J. M. and Van Ness, H. C. 'Introduction to Chemical Engineering Thermodynamics', 3rd Edn., McGraw-Hill, New York, 1975, p. 462
43 Symcox, R. O. and Ehrlich, P. *J. Am. Chem. Soc.* 1962, **84**, 531
44 Szabo, J., Luft, G. and Steiner, R. *Chem. Ing. Techn.* 1969, **41**, 1007
45 Takahashi, T. and Ehrlich, P. *Macromolecules* 1982, **15**, 714

46 Tatsukami, Y., Takahashi, T. and Yoshioka, H. *Makromol. Chem.* 1980, **181**, 1108
47 Thies, J. W., Doctoral Thesis, Technical University at Darmstadt, Germany, 1971
48 Tjahjadi, M., Gupta, A. K., Morbidelli, M. and Varma, A. *Chem. Eng. Sci.* 1987, **42**, 2385
49 Tobita, H. and Hamielec, A. E. *Makromol. Chem., Macromol. Symp.* 1988, **20/21**, 501
50 Tzoganakis, C., Vlachopoulos, J. and Hamielec, A. E. *Int. Polym. Process.* 1988, **III**, 141
51 Yamamoto, K. and Sugimoto, M. *J. Macromol. Sci.-Chem. (A)* 1979, **13**(8), 1067
52 Yoon, B. J. and Rhee, H.-K. *Chem. Eng. Commun.* 1985, **24**, 253
53 Budtov, V. P., Polyakov, Z. N., Gutin, B. L., Belayayev, V. M. and Ponomereva, Ye. L. *Polymer Science USSR.* 1982, **24**, 1367
54 Feucht, P., Tilger, B. and Luft, G. *Chem. Eng. Sci.* 1985, **40**, 1935

APPENDIX 1

DERIVATION OF MOMENT CLOSURE TECHNIQUE BY ASSUMING A LOG-NORMAL DISTRIBUTION

If we assume the molecular-weight distribution to be log-normal, then we will be able to solve the moment closure problem by expressing any integer moment of the distribution ($r > 2$) as a function of its lower moments.

The log-normal distribution is defined as:

$$f(x) = \frac{1}{\sqrt{(2\pi)}\sigma x} \exp\left(-\frac{(\ln x - \mu)^2}{2\sigma^2}\right) H(x) \quad \text{(A1.1)}$$

where $H(x)$ is the unit step function, or rather $H(x) = 1$ when $x > 0$ and $H(x) = 0$ for $x \leqslant 0$. μ and σ are parameters.

We define the rth moment of a variable x about the origin as:

$$m_r = \int_{-\infty}^{\infty} x^r f(x)\, dx$$

for log-normal distribution, it turns out to be:

$$m_r = \frac{1}{\sqrt{(2\pi)}\sigma} \int_0^{\infty} x^{r-1} \exp\left(-\frac{(\ln x - \mu)^2}{2\sigma^2}\right) dx$$

By using appropriate variable changes, the integral in the moment equation gives:

$$\int_0^{\infty} x^{r-1} \exp\left(-\frac{(\ln x - \mu)^2}{2\sigma^2}\right) dx = \sqrt{(2\pi)}\sigma \exp\left(\mu r + \frac{\sigma^2 r^2}{2}\right)$$

Following substitution in the moment equation, we finally obtain:

$$m_r = \exp(r\mu + \tfrac{1}{2}r^2\sigma^2) \quad \text{(A1.2)}$$

Note that the zeroth moment ($r = 0$) calculated from equation (A1.2) is unity, as it should be owing to the definition of probability density function $f(x)$. In order to satisfy this condition, we need to normalize the zeroth moment of the molecular-weight distribution, and the general result is given by:

$$Q_i^* = Q_i/Q_0 \quad \text{(A1.3)}$$

where the superscript * denotes the normalized moment.

Combining (A1.2) and (A1.3), one concludes:

$$m_i = Q_i^* = Q_i/Q_0$$

Note that:

$$m_i/m_j = Q_i^*/Q_j^* = Q_i/Q_j \quad \text{for all } i, j \quad \text{(A1.4)}$$

Now we want to evaluate the two parameters (μ and σ^2) in equation (A1.1) in terms of the moments. From equation (A1.2), setting $r = 1$ and 2 provides:

$$\ln Q_1^* = \mu + \tfrac{1}{2}\sigma^2 \qquad \ln Q_2^* = 2\mu + 2\sigma^2$$

Solving these two equations, one obtains

$$\mu = \ln(Q_1^{*2}/\sqrt{Q_2^*}) \quad \text{(A1.5)}$$

$$\sigma^2 = \ln(Q_2^*/Q_1^{*2}) \quad \text{(A1.6)}$$

In order to express any integer moment ($r > 2$) as a function of its lower moments, we need to find a relationship among the moments. From equation (A1.2):

$$\frac{Q_3^*}{Q_2^*} = \frac{\exp(3\mu + \frac{9}{2}\sigma^2)}{\exp(2\mu + 2\sigma^2)} = \exp(\mu + \tfrac{5}{2}\sigma^2) \quad \text{(A1.7)}$$

Substituting equations (A1.5) and (A1.6) into equation (A1.7), we get:

$$Q_3^* = (Q_2^*/Q_1^*)^3 \qquad Q_3 = (Q_2/Q_1)^3 Q_0 \quad \text{(A1.8)}$$

APPENDIX 2

A TEST OF THE MOMENT CLOSURE TECHNIQUES IN BRANCHING SYSTEMS

Introduction: the closure problem

It is becoming apparent that modelling of polymer molecular properties for systems where the polymer produced is not inert is becoming more and more important. Such systems involve branching and cross-linking to form a gel, peroxide attack in reactive extrusion, condensation reactions with multifunctional monomers and so on. In the more classical mathematical modelling of the molecular weights of the chains, as in free-radical polymerization, for example, the radicals grow to a certain length and are terminated by some mechanism, forming dead polymer chains. These chains are inert to further reaction. The production rate of these chains is only a function of the concentration of chains of smaller length. For these systems, one can readily calculate the entire chain-length distribution using the method of instantaneous molecular-weight distribution. Several systems of current interest now involve the case where radicals can attack this polymer to produce new radical centres at points along the backbone of the chain. This can produce long chain branching, or, if termination by combination is present, crosslinks leading to gel formation. Now the production rate of chains of a certain length depends upon the concentration of chains of all lengths, including those chains longer than the chain length of interest. This means that, in theory, in the first case one only needs to account for chains shorter than some maximum chain length, whereas, in the latter case, one must account for all chains from length unity to infinity.

One method of calculating the chain-length averages is the method of moments. In this technique, the leading moments of the chain-length distribution are calculated.

If we define the moments of the distribution to be:

$$Q_n = \sum_{r=0}^{\infty} r^n[\mathrm{P}(r)] + \sum_{r=0}^{\infty} r^n[\mathrm{R}(r)] \qquad \text{the } n\text{th moment}$$

and the averages are:

$$\bar{r}_n = Q_1/Q_0 \qquad \text{number average}$$
$$\bar{r}_w = Q_2/Q_1 \qquad \text{weight average}$$
$$\bar{r}_z = Q_3/Q_2 \qquad z \text{ average}$$

In this special case the moments of the distribution all depend upon the lower moments, i.e.

$$Q_n = f(Q_n, Q_{n-1}, Q_{n-2}, \ldots, Q_0)$$

In general, this need not be the case and we could have the case where:

$$Q_n = f(Q_\infty, \ldots, Q_{n+2}, Q_{n+1}, Q_n, Q_{n-1}, Q_{n-2}, \ldots, Q_0)$$

This means that one may have to calculate an infinite number of moments, certainly an impossible task. This is the closure problem.

The solution of Hulburt and Katz

A solution to this closure problem is to find an empirical equation to evaluate the higher moments as a function of the lower ones. One such method that has been used by several authors (including Kiparissides and Mavridis[29,33], Saidel and Katz[28,38], Chen *et al.*[8] and in slightly modified form Tzoganakis *et al.*[50]) was derived by Hulburt and Katz[26] based upon fitting the distribution by the first term of a Laguerre series. The closure formula is of the form:

$$Q_3 = \frac{Q_2}{Q_1 Q_0}(2Q_2Q_0 - Q_1^2)$$

This short appendix is to evaluate the usefulness of the Hulburt–Katz closure technique and compare it to the log-normal technique presented in this paper. To this end we shall derive the leading moments of the molecular-weight distribution for a simple free-radical reaction system, which is closed, and compare the results calculated by the moment equations and by the closure technique.

The kinetic example

Consider the following simple polymerization mechanism. Decomposition of initiator:

$$\mathrm{I} \xrightarrow{k_d} 2\mathrm{R}(1)$$

Propagation:

$$\mathrm{R}(r) + \mathrm{M} \xrightarrow{k_p} \mathrm{R}(r+1)$$

Termination by disproportionation:

$$\mathrm{R}(r) + \mathrm{R}(s) \xrightarrow{k_{td}} \mathrm{P}(r) + \mathrm{P}(s)$$

Termination by combination:

$$\mathrm{R}(r) + \mathrm{R}(s) \xrightarrow{k_{tc}} \mathrm{P}(r+s)$$

Transfer to monomer:

$$\mathrm{R}(r) + \mathrm{M} \xrightarrow{k_{fm}} \mathrm{P}(r) + \mathrm{R}(1)$$

where I is an initiator molecule, M is a monomer molecule, R(r) is a radical of length r, and P(s) is a dead polymer chain of length s.

One can also consider radical transfer to polymer, and propagation with internal double bonds, the branching reactions. Transfer to polymer:

$$\mathrm{R}(s) + \mathrm{P}(r) \xrightarrow{k_{fp}} \mathrm{P}(s) + \mathrm{R}(r)$$

Propagation with internal double bond:

$$\mathrm{R}(r) + \mathrm{P}(s) \xrightarrow{k_p} \mathrm{R}(r+s)$$

Mathematics. Defining the moments as:

$$Y_n = \sum_{r=0}^{\infty} r^n[\mathrm{R}(r)] \qquad \text{polymer radical moments}$$

$$X_n = \sum_{r=0}^{\infty} r^n[\mathrm{P}(r)] \qquad \text{dead polymer moments}$$

$$Q_n = Y_n + X_n \qquad \text{total macromolecule moments}$$

one can derive moment equations for the molecular-weight distribution. We can use the stationary-state hypothesis for the radical moments and assume that $Y_n \ll X_n$ such that $Q_n \simeq X_n$. One can write an expression for the moments of the polymer distribution, when transfer to polymer and propagation with internal double bonds are important. These equations are outlined by Tobita and Hamielec[49]:

$$\frac{1}{V}\frac{\mathrm{d}(VQ_0)}{\mathrm{d}x} = [\mathrm{M}_0]\left(\tau' + \frac{\beta}{2} - C^*_{p1}\right)$$

$$\frac{1}{V}\frac{\mathrm{d}(VQ_1)}{\mathrm{d}x} = [\mathrm{M}_0]$$

$$\frac{1}{V}\frac{\mathrm{d}(VQ_2)}{\mathrm{d}x} = [\mathrm{M}_0]\left(\frac{2(1+C^*_{p2})(1+C_{p2}+C^*_{p2})}{\tau'+\beta+C_{p1}} + \beta\frac{(1+C_{p2}+C^*_{p2})^2}{(\tau'+\beta+C_{p1})^2}\right)$$

$$\frac{1}{V}\frac{\mathrm{d}(VQ_3)}{\mathrm{d}x} = [\mathrm{M}_0]\left(1 + 3(1+C^*_{p2})\frac{Y_2}{Y_0} + 3(1+C^*_{p3})\frac{Y_1}{Y_0} + 3\beta\frac{Y_1Y_2}{Y_0^2}\right)$$

The radical moments are given by:

$$Y_0 = \{(2fk_d[\mathrm{I}])/(k_{tc}+k_{td})\}^{1/2}$$

$$Y_1 = \left(\frac{1+C_{p2}+C^*_{p2}}{\tau'+\beta+C_{p1}}\right)Y_0$$

$$Y_2 = \left(\frac{1+C_{p3}+C^*_{p3}}{\tau'+\beta+C_{p1}} + \frac{2(1+C^*_{p2})(1+C_{p2}+C^*_{p2})}{(\tau'+\beta+C_{p1})^2}\right)Y_0$$

where

$$\tau' = \frac{k_{td}Y_0}{k_p[\mathrm{M}]} + \frac{k_{fm}}{k_p} \qquad \beta = \frac{k_{tc}Y_0}{k_p[\mathrm{M}]}$$

and transfer to polymer:

$$C_{pi} = \frac{k_{fp}Q_i}{k_p[\mathrm{M}]}$$

propagation with internal double bonds:

$$C^*_{pi} = \frac{k^*_pQ_i}{k_p[\mathrm{M}]}$$

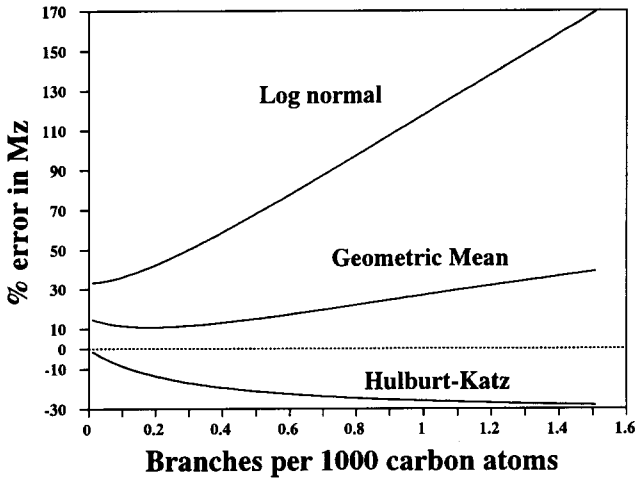

Figure 18 The effect of branching frequency on the error in M_z

The total number of trifunctional branch points, as generated by transfer to polymer, is given as:

$$\frac{1}{V}\frac{d(Q_0 B_{N3})}{dx} = [M_0]C_{p1}$$

B_{N3} is the number of trifunctional branch points per polymer molecule. We define conversion as:

$$x = (M_0 - M)/M_0$$

where M_0 is the initial monomer concentration. We can write

$$dx/dt = k_p Y_0 (1 - x)$$

We can solve these differential equations above (using a package LSODE) from $x = 0$ to $x = 1$ to give us the moments of the molecular-weight distribution.

The test

The conditions. Since we have a mathematically closed set of equations, we can calculate M_z and compare it to the value given by the closure techniques. For this test the temperature was isothermal, transfer to monomer was neglected and termination was all by disproportionation. When transfer to polymer is considered, and termination is by combination, the polymer tends to form a gel as indicated by Q_2 growing to infinity. Furthermore, propagation with internal double bonds tends to form a gel. Gel formation was avoided in this study by neglecting termination by combination and propagation with internal double-bond reactions.

We shall assume a constant reaction volume of one litre. The parameter values were adjusted to give polymer properties similar to those measured for low-density polyethylene[15] and thus:

$k_p = 26.2$ $\quad k_{td} = 12.6$ $\quad k_{fm} = 0$

$k_d = 4.3 \times 10^{-2}$ $\quad k_{tc} = 0$ $\quad k_{fp}/k_p = 2.0 \times 10^{-2}$

$M_0 = 10$ and $I_0 = 0.01 \times M_0$ mol l^{-1} (and constant). The maximum conversion was 25%. This gave the chain properties

$M_n = 20900$ $\quad M_z = 377000$

$M_w = 146000$ $\quad \lambda_{LCB} = 1.51$

It should be noted that the polydispersity of LDPE is not totally due to the long chain branching (as in this example), but also to the widely varying temperature and initiator levels experienced in a tubular reactor.

The effect of transfer to polymer (long chain branching). The effect of the transfer to polymer rate on the error between M_z and M_z calculated using the closure methods is shown in *Figure 18*. The branching frequency, λ_N, is presented as the number-average number of branches per 1000 carbon atoms. The error is calculated as:

$$\text{Error}(\%) = 100 \times \frac{M_{z(\text{closure})} - M_{z(\text{actual})}}{M_{z(\text{actual})}}$$

One can see that the log-normal method greatly overpredicts the M_z value for all branching frequencies but especially at higher branching frequencies. The Hulburt and Katz method gives very good results at low branching frequencies but tends to underpredict the M_z value at higher branching frequencies. The geometric mean error is, for the most part, less than that for either the log-normal or the HK method but has comparable absolute error as that of the HK method at the higher branching frequencies.

Conclusions

The closure technique of Hulburt and Katz seems to be adequate for narrow unbranched distributions but as the distribution broadens the error increases. The technique does not perform as well where there is significant branching, at least by transfer to polymer. In our example here we tried to simulate polymer properties near that measured for HP–LDPE and found the error to be quite significant. Nevertheless for this example the Hulburt and Katz method is superior to the log-normal method. In polyethylene production at temperatures near 300°C, β-scission may be important, and would tend to narrow the distribution possibly helping to keep the error in the Hulburt and Katz method within tolerable limits. One must be cautious when choosing a closure technique, since the adequacy of the technique must depend a great deal on the shape of the molecular-weight distribution, and on how it changes with conversion.

APPENDIX 3

SUMMARY OF SOME RECENT ATTEMPTS AT MODELLING LDPE TUBULAR REACTORS

Authors	*Reactions included*	*Parameters from*	*Comments*
Agrawal and Han (1975)[2]	Peroxide initiation Combination Transfer to monomer Transfer to polymer Transfer to transfer agent β-scission	From literature data (Agrawal 1974)[1]	Studied axial mixing

Chen *et al.* (1976)[8]	Peroxide initiation Combination Transfer to polymer β-scission	*Rate:* Ehrlich and Mortimer (1970)[11] *MWD:* to give reasonable values	Suggest neglect axial mixing Let reaction mixture properties vary with reactor length Scission or transfer necessary to obtain reasonable *MWD*
Han and Liu (1977)[22]	Peroxide initiation Combination Transfer to monomer Transfer to polymer Transfer to transfer agent β-scission	Agrawal and Han (1975)[2]	Multiple injections of monomer and initiator
Lee and Marano (1979)[3]	Peroxide initiation Combination Disproportionation Transfer to monomer Transfer to polymer Transfer to transfer agent	Szabo and Luft (1969)[44] Ehrlich and Mortimer (1970)[11] Assumed activation volumes	Did not use s.s.h. for radicals Used model for sensitivity study and to show trends
Goto *et al.* (1981)[17]	Peroxide initiation Termination Transfer to monomer Transfer to polymer Transfer to transfer agent β-scission of sec radical β-scission of tert radical Backbiting	From experiment in a vessel reactor Termination rate by assuming segmental diffusion	Extensive comparison with experimental data
Budtov *et al.* (1982)[53]	Oxygen initiation Disproportionation Transfer to monomer Transfer to polymer Transfer to propane	From experiment in a tube Symcox and Ehrlich (1962)[43]	Used oxygen initiation (first order w.r.t. oxygen)
Donati *et al.* (1982)[10]	Peroxide initiation Oxygen initiation Combination Disproportionation		No molecular-weight calculations Pulse valve effect on axial mixing negligible, based on fluid dynamic measurements
Hollar and Ehrlich (1983)[25]	Peroxide initiation Oxygen initiation Thermal self-initiation Termination β-scission	Chen *et al.* (1976)[8] Takahashi and Ehrlich (1982)[45]	Included thermal self-initiation of ethylene Concluded that oxygen behaves as a fast and a slow initiator
Yoon and Rhee (1985)[52]	Peroxide initiation Termination Transfer to monomer Transfer to polymer	Chen *et al.* (1976)[8] Lee and Marano (1979)[31]	Studied axial mixing and concluded it may be neglected Studied s.s.h. for radicals and concluded it is a valid assumption Studied optimal temperature profiles
Mavridis and Kiparissides (1985)[29,33]	Peroxide initiation Combination Disproportionation Transfer to monomer Transfer to polymer Transfer to transfer agent β-scission	Lee and Marano (1979)[31]	Tested s.s.h. for radical concentration and concluded it is a valid assumption Included momentum balance to calculate pressure Performed sensitivity study to optimize performance Multiple initiators

Shirodkar and Tsien (1986)[39]	Peroxide initiation Combination Disproportionation Transfer to monomer Transfer to polymer Transfer to transfer agent β-scission Backbiting	Plant data	Two reaction zones with multiple initiator and monomer feeds
Gupta *et al.* (1987)	Peroxide initiation Termination Transfer to polymer Transfer to transfer agent β-scission of sec radical β-scission of tert radical Backbiting	Chen *et al.* (1976)[8] Goto *et al.* (1981)[17]	Conclude that s.s.h. for radical concentrations valid Multiple initiator and monomer feeds
Tjahjadi *et al.* (1987)[48]	Peroxide initiation Combination	Laurence and Pottiger (1985)[30]	Sensitivity analysis performed
Brandolin *et al.* (1988)[5]	Oxygen initiation Combination Transfer to polymer Transfer to transfer agent β-scission	Rate parameters from reactor temperature profile Molecular-weight parameters to match measured molecular properties	Oxygen initiation modelled as nth-order reaction (w.r.t. oxygen), $n = 1.1$
This work	Peroxide initiation Oxygen initiation Oxygen retardation and re-initiation Thermal self-initiation Combination Disproportionation Transfer to monomer Transfer to polymer Transfer to transfer agent β-scission of terminal radicals β-scission of backbone radicals Backbiting	Industrial reactor temperature profile and final conversion Measured molecular weights Reasonable branching frequencies	Allows for copolymerization Accounts for pulse valve pressure variation Oxygen initiation, retardation and re-initiation Multiple initiators Multiple feed points